

TWIX: Automatically Reconstructing Structured Data from Templatized Documents

Yiming Lin, Mawil Hasan, Rohan Kosalge, Alvin Cheung, Aditya G. Parameswaran
yiminglin | mawil0721 | rohankosalge | adityagp@berkeley.edu, akcheung@cs.berkeley.edu
UC Berkeley

ABSTRACT

Many documents, that we call *templated documents*, are programmatically generated by populating fields in a visual template. Effective data extraction from these documents is crucial to supporting downstream analytical tasks. Current data extraction tools often struggle with complex document layouts, incur high latency and/or cost on large datasets, and often require significant human effort, when extracting tables or values given user-specified fields from documents. The key insight of our tool, TWIX, is to predict the underlying template used to create such documents, modeling the visual and structural commonalities across documents. Data extraction based on this predicted template provides a more principled, accurate, and efficient solution at a low cost. Comprehensive evaluations on 34 diverse real-world datasets show that uncovering the template is crucial for data extraction from templated documents. TWIX achieves over 90% precision and recall on average, outperforming tools from industry: Textract and Azure Document Intelligence, and vision-based LLMs like GPT-4-Vision, by over 25% in precision and recall. TWIX scales easily to large datasets and is 734× faster and 5836× cheaper than vision-based LLMs for extracting data from a large document collection with 817 pages.

1 INTRODUCTION

Many real-world documents are generated from structured data by programmatically filling fields in a *visual template* [37, 47], such as tax forms, invoices, grant reports, pay stubs, certification records, and order bills. Figure 1 shows an example from police complaint records provided by our journalism collaborators¹. In this example, Record 1 and 2 are visually similar because they were generated from structured data using the same template². However, the templates used to create these documents are typically inaccessible. We refer to documents generated from the same template as *templated documents*, and refer to a *record* as an instance created by populating fields from a given template.

Templated documents present information in a semi-structured, form-like layout, where data is organized in tables or key-value blocks. Accurate data extraction from such documents is crucial for supporting various downstream analytical tasks. Consider a journalist who wants to determine *the names of officers mentioned in complaints after 06/01/2023, with the complaint description as Rude Conduct* by analyzing documents such as those in Figure 1. Or, an analyst may seek to find *the total rates of events of type NM in September* by examining invoices such as those in Figure 2.

¹We collaborate with Big Local News at Stanford and the Investigative Reporting Program at Berkeley, as well as the California Reporting Project, a consortium of 30+ newsrooms in California.

²There are thousands of records generated using this same template. Here, we present only two examples for illustration.

Unfortunately, data extraction from real-world templated documents is challenging because of complex layouts. Templated documents often contain a mix of blocks with different visual patterns (table or key-value). The documents in Figure 1 and Figure 2 consist of both table and key-value portions. Each pattern requires a distinct approach for extracting the corresponding data. For example, in a table block, fields are typically arranged in the first row (e.g., {Date, Number, ...}), with corresponding values in each column. In contrast, a key-value block usually places the field and its value horizontally within a row (e.g., Gender and FEMALE). Visual cues implicitly signal relationships between fields and values. Furthermore, different data blocks may be arranged in a nested structure. In Figure 2, several small tables (e.g., blocks B_3 and B_4) are nested within a larger table, block B_2 . Additionally, documents often include headers, footers, and free text—while these elements may not be part of the template, they are often important and need to be extracted alongside the structured data.

Point extraction methods are insufficient. Data extraction from documents, be it templated, or otherwise, is not new. One line of research [10, 37, 40, 43, 47, 48] focuses on extracting values based on user-specified or predefined fields, which we refer to as *point extraction*, e.g., extracting the value for the field Date in Figure 1. Point extraction methods face several significant limitations when applied to real-world documents. First, the given fields are extracted in isolation, missing global understanding in the form of *relationships* between the extracted data across fields. This makes them unsuitable for downstream analysis involving multiple fields. For instance, directly applying point extraction to the document in Figure 1 would result in long lists of values for the given fields (e.g., Date, Name) shown to the right of the police records. Relationships between fields, such as types of complaints and their corresponding dispositions are lost. Furthermore, fields in the document (e.g., Start Date in Figure 2) may not be unique, leading to ambiguous results from point extraction. Second, most point extraction methods [10, 47, 48] train deep learning models based on labeled documents created with a specific template and then applied to others that use the same template. Unfortunately, human effort quickly adds up as the number of extracted fields and templates in the document set increases.

Industry extraction APIs and vision LLMs are error-prone. Yet another data extraction approach involves tools from industry based on pretrained text or vision models—such as AWS Textract [1] or Azure Document Intelligence [2]—which offer general-purpose capabilities to extract structured data, such as tables or key-value pairs, from documents. Or alternately to use vision-based LLMs [6] (e.g., OpenAI GPT-4 Vision) directly, which can be prompted to do the same. However, these approaches struggle with the complex and heterogeneous layouts in real-world documents, leading to sub-optimal performance, plus non-trivial cost and latency. For

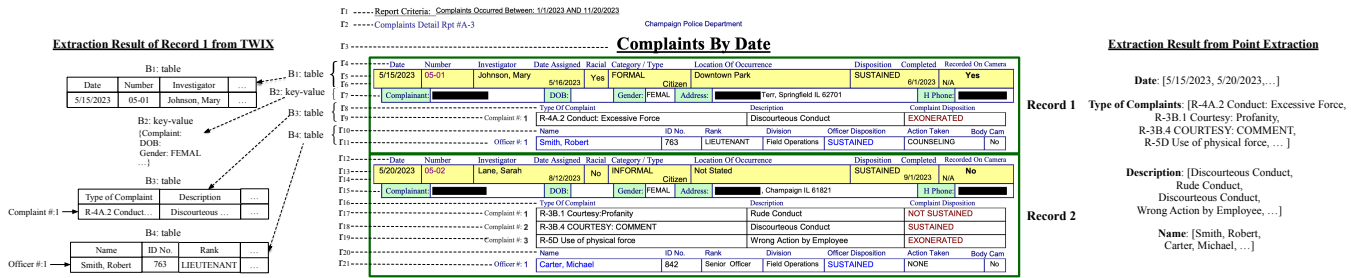


Figure 1: Police complaint records provided by our journalism collaborators. (Actual values have been replaced for privacy.) Row indices $[r_1, r_2, \dots]$ and block labels $[B_1, B_2, \dots]$ are manually annotated, where B stands for a data block.

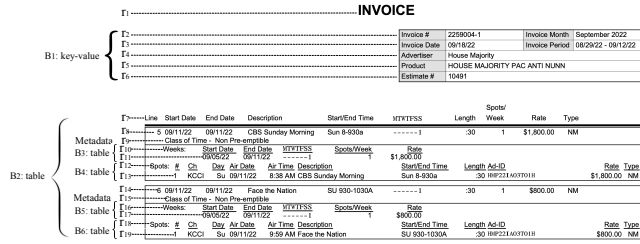


Figure 2: Portions of a Record in an Invoice Document from the Open Benchmark. Row indices $[r_1, r_2, \dots]$ and block labels are manually annotated.

example, these approaches have difficulty with settings such as Figure 1, which has data blocks with different patterns mixed together, or Figure 2, which has two small tables (e.g., B_3 and B_4) nested under a larger table (e.g., B_2). On our benchmark of 34 real-world datasets, these tools achieved precision and recall between 55% and 65%, while our approaches achieved over 90% precision and recall. Finally, while we could also consider web data extraction approaches, these don't apply to our setting due to the lack of HTML tags explicitly indicating hierarchical relationships. We discuss all these approaches in detail in Section 6.

TWIX: Inferring templates prior to extraction. In this paper, to extract data from templated documents, our tool, TWIX³, first reconstructs the template from a set of documents generated using the same template, and then extracts data from the documents. The extraction result of Record 1 in Figure 1 is shown on the left, beginning with a table block B_1 , followed by a key-value block B_2 , and two additional table blocks B_3 and B_4 . Unlike point extraction, TWIX extracts all structured data from documents, providing a global context for end users to perform ad-hoc analysis on fields of interest. Unlike pre-trained learning-based approaches that attempt to directly extract structured data from documents, our key insight is to predict the underlying template used to generate templated documents. This template serves as the backbone of the documents, making downstream template-based data extraction more logical, efficient and effective.

Inferring the template. While the idea of inferring a visual template and then using it for extraction is intuitively appealing, doing so presents challenges in two fronts: *field prediction*, i.e., predicting which fields are phrases, and *template assembly*, i.e., assembling the fields into a template that was used to generate records.

Challenge 1: Predicting fields. Unfortunately, it's not even clear which phrases in a document may be fields, and which may be values. If a document contains only tables, it's straightforward to

³Short for Templated document Wrangling for Information eXtraction.

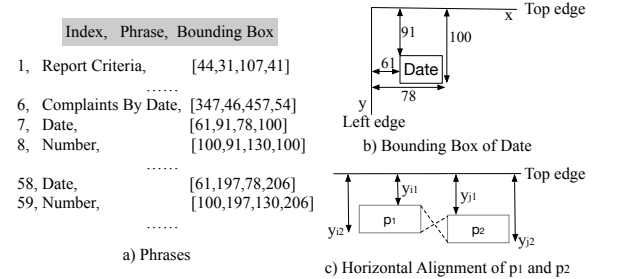


Figure 3: Extracted Phrases and Bounding Boxes in Police Records.

determine the fields, as they correspond to the headers of these tables. However, most real-world documents go beyond tables, as in Figure 1 and 2, which contain a mix of nested key-value and tabular blocks, interspersed with other metadata. So while there are visual indicators that are easy for a human to understand, e.g., vertical or horizontal alignment, proximity of value phrases to key ones, or indentation, these are hard to develop robust rules around. Our key insight here is that *fields appear in similar positions across records*, e.g., {Date, Number, ...} in Figure 1. Consider the phrases extracted from police complaint by OCR tools [5] in Figure 3-a, where the phrase index indicates the order of extraction (e.g., Report Criteria and Date in Record 1 are the 1st and 7th extracted phrases, with indexes 1 and 7). For fields like Date and Number, the difference in their indexes in every record is consistently 1, since records are created using the same template. Among all phrases in the document, only a small subset (corresponding to fields) exhibit the consistent position pattern or “gap” as described above, while most values (e.g., 05-01) appear randomly across records. While this positional “gap” pattern may appear in records without nesting, nesting raises additional idiosyncrasies, meriting relaxation of the criteria above. In cases where visual cues prove insufficient, we can further use LLMs to improve the robustness of our approach using their semantic knowledge to predict fields. Here, instead of asking LLMs to handle complex tasks like recognizing intricate visual layouts or structures within documents, we limit their role to simpler tasks by providing straightforward context (e.g., by asking “Is this phrase a field or a value?”), resulting in higher prediction accuracy.

Challenge 2: Assembling the template. Predicting fields alone is insufficient to capture the template, as we not only have a similar problem as in point extraction of not knowing which fields are related to which other fields, but also how they are organized to form records. Our key insight here is that a record often consists of multiple data blocks, such as table or key-value blocks, and the placement of data blocks follows a consistent pattern across records.

For instance, each police complaint has four blocks arranged sequentially: a table block, followed by a key-value block, and then two more table blocks. We refer to the placement of data blocks as the template structure, formally defined in Section 2. To predict such a structure, TWIX assigns each row a label in the record to one of four categories, {Key, Key-Value, Value, Metadata}, each associated with a probability estimated based on the predicted fields. We formulate the row labeling problem as an optimization problem that finds the most probable label assignments for the rows (i.e., maximizing the product of probabilities per row), constrained by the validity of the table structure (e.g., a Key row must have a vertically-aligned Value row beneath it, and vice versa). We prove this *row labeling problem* to be **NP-hard**, and we present efficient approximate approaches to find the row labels, based on which we further learn the tree structure of the template (Section 3.3). The template for police complaints is shown in Figure 4-1, where the four leaf nodes represent the four data blocks, arranged from left to right to indicate their order of appearance. Each node contains the set of predicted fields and its type (e.g., table or key-value).

Data extraction using the template. The template tells us how records are generated by filling in the predicted fields. So, we first divide the documents into a list of records, each created from the same template (Section 4.1). Each record is then separated into a tree of data blocks based on the template (Section 4.2). Data extraction is then performed within each data block, with different patterns implying distinct extraction logic based on the block type (Section 4.3). For instance, a table block (e.g., B_1 , B_3 , and B_4 in Figure 1) typically places headers in a row, with corresponding values organized in columns, whereas key-value blocks (e.g., B_2) tend to arrange fields and its values horizontally in a row.

Overall, we make the following contributions as part of developing TWIX, a robust tool for data extraction from documents.

- We introduce the concept of a *template* for templated documents (Section 2) and propose novel algorithms to infer the template (Section 3). Specifically, we develop a graph-based algorithm leveraging location vectors encoding visual information, coupled with LLM invocations, to predict fields (Section 3.1). We formulate the problem of labeling rows based on whether they belong to a key-value or table block or are metadata, and show NP-hardness, with an efficient solution to further predict the template (Section 3.2).
- We present robust unsupervised data extraction techniques capable of handling data blocks with different structural patterns (Section 4). We first divide documents into records (Section 4.1), and then further split each record into a list of data blocks (Section 4.2), both guided by the predicted template. Robust data extraction is then performed within each data block (Section 4.3). We further provide theoretical error bounds and correctness guarantees (Section 4.4).
- We collected 34 diverse real-world datasets and conducted a comprehensive evaluation, comparing our approach against four state-of-the-art techniques (Section 5). TWIX achieves approximately 90% precision and recall, **outperforming the baselines by over 25%** in both metrics. TWIX scales efficiently to large datasets, being **734× faster and 5836× cheaper** than vision-based LLMs for extracting data from a large document collection with 817 pages.

2 PROBLEM FORMULATION

2.1 Preliminaries

Consider a dataset $\mathcal{D} = \{D_1, D_2, \dots\}$, where D_i is a document. For simplicity, we denote D to be the *concatenation* of all the documents in \mathcal{D} , i.e., $D = [D_1, D_2, \dots, D_n]$ in some order. We focus on the setting where D consists of records created using the same template (e.g., Records 1 and 2 in Figure 1) and other metadata (e.g., headers, footers), where the concepts of record, template, and metadata are defined shortly. This is typical in many real-world settings, e.g., invoices, tax documents, and immigration forms.

We operate on the serialized plain text representation of this concatenated document D . Let P be the phrases extracted from D by using OCR tools [5, 8],⁴ in ascending order of position, i.e., $P = [p_1, p_2, \dots, p_m]$. Figure 3-a presents phrases extracted from the police complaint document in Figure 1. Each phrase p_i is paired with its bounding box $b_i = [x_{i1}, y_{i1}, x_{i2}, y_{i2}]$ shown in Figure 3-a. Here, x_{i1} and x_{i2} represent distances from the left and right edges of p_i to the left edge of the page, respectively. Similarly, y_{i1} and y_{i2} denote distances from the top and bottom edges of p_i to the top edge of the page, respectively. Figure 3-b presents the bounding box of the first Date (Date in Record 1). Each phrase p_i has its positional *index* i , i.e., its location in the document, denoted as $ind(p_i)$, determined by the OCR tool, which extracts phrases row-by-row, from left to right, shown in Figure 3-a. For instance, Report Criteria and Date (in Record 1 in Figure 1) are the first and sixth phrases extracted with index 1 and 6, respectively.

We next define the concept of *rows*, to be used in template prediction in Section 3. Consider phrases p_i and p_j with bounding boxes $[x_{i1}, y_{i1}, x_{i2}, y_{i2}]$ and $[x_{j1}, y_{j1}, x_{j2}, y_{j2}]$, respectively. We denote $p_i \neq p_j$ if phrases p_i and p_j are visually *horizontally aligned* in the same row, i.e., $y_{i1} \leq y_{j2} \wedge y_{i2} \geq y_{j1}$. In Figure 3-c, $p_1 \neq p_2$. We use a loose definition of alignment allowing overlaps. Let $r_i = [p_{i1}, p_{i2}, \dots, p_{im}]$ be a row with a list of phrases, where $\forall p_{ik}, p_{il} \in r_i, p_{ik} \neq p_{il}$. We transform phrases $P = [p_1, p_2, \dots]$ to rows $R = [r_1, r_2, \dots]$ greedily by scanning $p_i \in P$ in increasing order of index. Phrase p_i is merged into an existing row r if $\forall p_j \in r, p_i \neq p_j$; otherwise, a new row is created for p_i . When a phrase p is horizontally aligned with multiple rows, such as “Yes”, the first value under column Racial in Figure 1, p is merged into the first row it is horizontally aligned with, e.g., Yes is part of r_5 instead of r_6 .

For any phrase $p \in P$, it can be assigned one of the labels from $\{field, value, metadata\}$. *Fields* refer to the column names of a table embedded in the document D or the keys in key-value pairs. A *value* is a phrase whose corresponding field can be identified, such as a cell in a table row or a value in a key-value pair. Note that the same phrase may appear multiple times in P (e.g., Date in police complaints appears in row r_4 and r_{12}). When we refer to *the field* p_j of a value p_i , we mean the field phrase p_j whose index j is largest subject to $j < i$, among all occurrences of that particular field phrase. For example, the field of 5/20/2023 corresponds to the Date at r_{12} rather than the earlier Date at r_4 .

Other non-field phrases whose fields cannot be identified are called *metadata*, such as the title “Complaints By Date”, or headers, e.g., phrases in row r_1 and r_2 in Figure 1. We assume that the label

⁴Our approach is suitable for documents where phrases and their bounding boxes can be extracted, such as PDFs, Word documents, and scanned images.

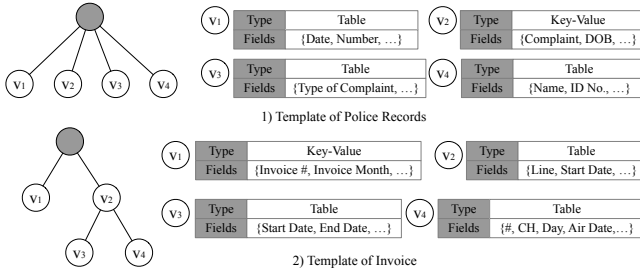


Figure 4: Templates for Police Records and Invoice Document.

for each phrase $p \in P$ is unique. For instance, a phrase cannot be both a field and the value of another field, a scenario that we rarely observe in real-world datasets.

2.2 Template Formulation

We now formally define the notation of a template. A document D consists of a set of *records*, each generated using the *template*. Each record recursively consists of *blocks* within D , which correspond to a sequence of rows. Let T be the *template* used to generate records, where $T = (V, E)$ is an ordered directed tree with an artificial root node. For each non-root node $v \in V - \{root\}$, v is associated with a *type*, $v.type \in \{Table, Key-Value\}$, and a set of *fields*, $v.fields$. In Figure 4, we present the templates for police complaints and invoices, respectively, where the type and fields for each node are specified. Intuitively, a template defines how a document is populated with records by specifying which fields are populated, in what manner (e.g., as a table or a key-value block), and order (e.g., which block appears first).

For a node $v_i \in V - \{root\}$, we denote $v_i \rightarrow B_i$ to be the process of generating a data block B_i by populating fields in v_i . B_i is a sequence of rows, where every *field* phrase in $v_i.fields$ appears exactly once in B_i and all of the *value* phrases that correspond to those field phrases appear in B_i . Let Rec_i be a record formed by populating fields from template T , comprising a sequence of data blocks generated by the nodes in T . To do so, each node v_i in T generates one or more data blocks in the predefined order in T , all as part of this record.

EXAMPLE 1. Block B_1 in the first police complaint record Rec_1 corresponds to $[r_4, r_5, r_6]$ in Figure 1. In its template shown in Figure 4-1, B_1 is generated by populating the fields from the table node v_1 in Figure 4-1. A single police complaint record then comprises one or more data blocks generated by each of v_1, v_2, v_3 and v_4 in that order. In Figure 2, blocks B_3 and B_5 in the invoice document are both generated by v_3 in Figure 4-2, while v_2 generates B_2 . Note that v_2 is the parent of v_3 , indicating that v_3 's data blocks $\{B_3, B_5\}$ are nested within v_2 's block B_2 , as we will discuss below. \square

Let \mathcal{B}_v^{Rec} be the set of blocks generated by the node v in the record Rec , i.e., $\mathcal{B}_v^{Rec} = \{B_i | v \rightarrow B_i, B_i \in Rec\}$. For example, in the police complaint record in Figure 1, $\mathcal{B}_{v_1}^{Rec_1} = \{B_1\}$, while $\mathcal{B}_{v_3}^{Rec_1} = \{B_3, B_5\}$ in the invoice document in Figure 2. Let $ind(\mathcal{B}_v^{Rec})$ be the index of \mathcal{B}_v^{Rec} , defined as the smallest index of phrase p in any block in \mathcal{B}_v^{Rec} , i.e., $ind(\mathcal{B}_v^{Rec}) = \min ind(p), p \in B_i, \forall B_i \in \mathcal{B}_v^{Rec}$.

Two data blocks may overlap (e.g., B_2 and B_3 in Figure 2), while others may not (e.g., B_1 and B_2 in Figure 1). To formally define overlapping relationships between data blocks, for two blocks B_i and B_j , we denote $B_i \cap B_j = \emptyset$ if $\forall p_{i_1}, p_{i_2} \in B_i$ and $p_{j_1}, p_{j_2} \in B_j$, such

Data	Phrase	Vector	
First 5 Records in Police Complaints	Date	[7,58,128,195,251]	$M, \Delta=1$
	Number	[8,59,129,196,252]	
	5/15/2023	[17]	$M, \Delta=1$
	05/01	[18]	
	Type of Complaint	[34,85,155,222,278]	
First 5 Records in Invoices	Description	[35,86,156,223,279]	$M, \Delta=1$
	No	[74,78,126,140,142,144,187,...]	
	Line	[16,126,251,381,503]	PM $M, \Delta=1$
	Start Date	[17,39,84,127,149,194,252,...]	
	End Date	[18,40,85,128,150,195,253,...]	

Figure 5: Location Vectors of Sample Phrases in First 5 Records in Police Complaints and Invoices.

that $(i_1 > j_1) \oplus (i_2 > j_2) = 0$, where i_1, i_2, j_1, j_2 are phrase indexes, and \oplus denotes the logical XOR operation. Otherwise, $B_i \cap B_j \neq \emptyset$. Intuitively, $B_i \cap B_j = \emptyset$ implies that the visual bounding boxes of the two blocks do not overlap, such as any two blocks in the police complaints records. In the invoice records in Figure 2, $B_1 \cap B_2 = \emptyset$, while $B_2 \cap B_3 \neq \emptyset$ since phrases from B_2 are placed both before and after B_3 , e.g., row r_8 appears before B_3 , while row r_{14} appears after B_3 . Given a record Rec , and $v_i, v_j \in V_d$, we denote $\mathcal{B}_{v_i}^{Rec} \cap \mathcal{B}_{v_j}^{Rec} = \emptyset$ if $\forall B_i \in \mathcal{B}_{v_i}^{Rec}, B_j \in \mathcal{B}_{v_j}^{Rec}, B_i \cap B_j = \emptyset$.

Now we describe how edges in the template T influences overlap of data blocks. For any two nodes $v_i, v_j \in V - \{root\}$, when v_i is an *ancestor* of v_j , then $\forall Rec, ind(\mathcal{B}_{v_i}^{Rec}) < ind(\mathcal{B}_{v_j}^{Rec})$ and $\mathcal{B}_{v_i}^{Rec} \cap \mathcal{B}_{v_j}^{Rec} \neq \emptyset$. Likewise, when v_i is a *left sibling* of v_j , then $\forall Rec, ind(\mathcal{B}_{v_i}^{Rec}) < ind(\mathcal{B}_{v_j}^{Rec})$ and $\mathcal{B}_{v_i}^{Rec} \cap \mathcal{B}_{v_j}^{Rec} = \emptyset$.

EXAMPLE 2. As shown in Figure 4-1, the non-root nodes are placed at the same level from left to right, indicating that their corresponding data blocks B_1, B_2, B_3 , and B_4 for the given record do not overlap and appear in the pre-order traversal of the nodes in T . In contrast, the template for invoice records in Figure 4-2 shows that node v_2 is an ancestor of v_3 , implying that the data blocks of v_3 , $\mathcal{B}_{v_3}^{Rec} = \{B_3, B_5\}$, overlap with the data blocks of v_2 , $\{B_2\}$, and B_2 appears before B_3 and B_5 . Note that the sequence of data blocks corresponding to the subtree rooted at v_2 can be repeated, provided the sequence of data blocks for its children complies with the edge definition above. \square

Given the concepts of templates, data blocks, and records, we describe our tool, TWIX, which first predicts the template (Section 3), and then extracts data based on the learned template (Section 4).

3 TEMPLATE PREDICTION

We now describe how TWIX infers the template T given the concatenated document D populated with records generated by T .

3.1 Field Prediction

As a first step, TWIX predicts a set of fields given the extracted phrases P from document D . The key intuition we leverage is that the set of fields often appear in similar locations across records.

3.1.1 Location Vectors and Matches. Since the same phrase p (e.g., Date) may appear multiple times in P , such as p_7, p_{58} , we denote $v_p = [i, \dots, j]$ as the *location vector* of p , comprising the indexes of occurrences of p in ascending order. Table 5 lists the location vectors for sample phrases in the first five records in police complaints and

invoices. The phrase Date appears exactly once in each record, corresponding to the list of phrases $[p_7, \dots, p_{251}]$, and thus has the location vector $[7, \dots, 251]$. Let L_p be the length of the vector v_p .

To formalize the intuition that two related fields p_i and p_j share similar locations, we observe that their location vectors are often related by a constant shift. In Table 5, adding one to each entry in the location vector for Date aligns it with the location vector for Number. This is because Date and Number are fields in the same table node, and thus appear in sync in the blocks corresponding to that node, resulting in constant relative distances across records. We define the concept of *perfect match* to capture this observation.

DEFINITION 1. PERFECT MATCH. Let $v_{p_i} = [i_1, i_2, \dots]$ and $v_{p_j} = [j_1, j_2, \dots]$ be the location vectors of phrases p_i and p_j . We say p_i is a *perfect match* with p_j , denoted by $M(v_{p_i}, v_{p_j}) = 1$, if $L_{p_i} = L_{p_j}$, $L_{p_j} > 1$ and $\exists \Delta$, s.t., $\forall i_k \in v_{p_i}, j_k \in v_{p_j}, |i_k - j_k| = \Delta$.

When $L_{p_j} = 1$, any two phrases will be a perfect match, and thus we enforce $L_{p_j} > 1$ above. We further relax this notion below.

DEFINITION 2. PARTIAL PERFECT MATCH. Let $v_{p_i} = [i_1, i_2, \dots]$ and $v_{p_j} = [j_1, j_2, \dots]$ be the location vectors of phrases p_i and p_j . We say p_i is a *partial perfect match* with p_j , denoted by $PM(v_{p_i}, v_{p_j}) = 1$, if there exists a subsequence $v'_{p_i} \subseteq v_{p_i}$, $M(v'_{p_i}, v_{p_j}) = 1$.

EXAMPLE 3. In Table 5, any pair of phrases among Date, Number, Type of Complaint and Description is a perfect match, while 5/15/2023, 05/01 and No are not a perfect match with any other phrases. In Figure 2, the same field, such as Start Date, may appear in multiple blocks (e.g., B_2, B_3 and B_5) within a record, while some phrases, such as Line, only appear in a unique block (e.g., B_2). In this case, Line is a partial perfect match with Start Date because a subsequence of the location vector for Start Date perfectly matches Line. This subsequence corresponds to the appearances of Start Date in B_2 every record. \square

Next, we present two properties of the match functions above to illustrate their effectiveness in predicting fields. Given document D , let $T' = (V', E')$ be the *true* template for D , and let F' be the corresponding set of fields. A field $p \in F'$ is called a *true* field.

PROPOSITION 1. Given the true template $T' = (V', E')$, when there exists a unique node $v \in V'$, $v.type = table$, $p_i, p_j \in v.fields$, if $L_{p_i} = L_{p_j}$, then p_i and p_j are a perfect match; if $L_{p_i} > L_{p_j}$, then p_j and p_j are a partial perfect match.

Proposition 1 states that if phrases p_i and p_j are both fields of a unique table node in T' (e.g., Date and Number in police complaints), and their location vectors have the same length, they must be a perfect match. This is because records are generated using the same T' , ensuring that the relative distance between p_i and p_j remains constant across all records. Conversely, when their location vectors have different lengths, such as $L_{p_i} > L_{p_j}$, field p_i (e.g., Start Date in invoices) may appear in multiple nodes, while p_j (e.g., Line) belongs only to v . In this case, v_{p_j} and the subsequence of p_i 's location vector corresponding to its occurrences in blocks generated by node v , denoted as v'_{p_i} , must be a perfect match since v'_{p_i} and v_{p_j} share the same vector length. A proof of Proposition 1 is shown below.

PROOF OF PROPOSITION 1. In the true template $T' = (V', E')$, when there exists a unique node $v \in V'$, $v.type = table$, $p_i, p_j \in v.fields$, if $L_{p_i} = L_{p_j}$, we have $\nexists v' \in V', v \neq v',$ s.t., $p_i \in v'.fields$ or $p_j \in v'.fields$, under the assumption that we make that each

phrase p has a unique label. Otherwise, $L_{p_i} \neq L_{p_j}$. Let the location vectors of p_i and p_j be $v_{p_i} = [i_1, i_2, \dots, i_m]$, $v_{p_j} = [j_1, j_2, \dots, j_m]$, respectively. $\forall B_k$, where $v \rightarrow B_k$, let the index of p_i and p_j in B_k be i_k and j_k , respectively. $\forall k_1, k_2 \in [1, m]$, we have $i_{k_1} - j_{k_1} = i_{k_2} - j_{k_2}$, since $v \rightarrow B_{k_1}$ and $v \rightarrow B_{k_2}$, and the schema of table in the template is consistent across the records. This completes the first half of proposition.

When $L_{p_i} > L_{p_j}$, let v'_{p_i} be the subsequence of v_{p_i} that occurs in blocks created from v , i.e., $\forall p_k \in v'_{p_i}, p_k \in B$, where $v \rightarrow B$. Based on the above proof, v'_{p_i} is a perfect match with v_{p_j} , and thus v_{p_i} is a partial perfect match with v_{p_j} . \square

Next we establish the corresponding property for fields in a key-value node. Consider a true field p in a node v whose type is *Key-Value* in T' (e.g., DOB in police complaints). Let $f(p)$ be an indicator function where $f(p) = True$ if the corresponding value for p is always missing or always not-missing in every record generated by T' (e.g., Gender). Otherwise, $f(p) = False$.

PROPOSITION 2. Consider the true template $T' = (V', E')$. Given a unique node $v \in V'$, $v.type = Key-Value$, $p_i, p_j \in v.fields$, and $f(p_i) = f(p_j) = True$, if $L_{p_i} = L_{p_j}$, then p_i and p_j are a perfect match; if $L_{p_i} > L_{p_j}$, then p_j and p_j are a partial perfect match.

Proposition 2 states that if two phrases have a consistent filling pattern ($f(\cdot) = True$) in a unique key-value node, they must be a perfect match. For instance, if DOB's value is always missing while Gender's value is always present in every record, then DOB and Gender are a perfect match, provided their location vectors have the same length. Conversely, if $f(p_i) = False$, the relative distance between p_i and p_j is not consistent across records. However, even in this case, the phrase p_i with $f(p_i) = False$ ends up being a partial perfect match with phrase p_j (where $f(p_j) = True$) if there exists a sequence of two data blocks in which p_i is either consistently "present" or consistently "missing," a scenario commonly observed in practice.

A proof is presented below.

PROOF OF PROPOSITION 2. Consider the location vectors of p_i and p_j , $v_{p_i} = [i_1, i_2, \dots, i_m]$, $v_{p_j} = [j_1, j_2, \dots, j_m]$. Under the assumption that a phrase p has a unique label, when there exists a unique node $v \in V'$, $v.type = Key-Value$, $p_i, p_j \in v.fields$, and $f(p_i) = f(p_j) = True$, if $L_{p_i} = L_{p_j}$, $\forall B_k, v \rightarrow B_k$, let the index of p_i and p_j in B_k be i_k and j_k , respectively.

$\forall k_1, k_2 \in [1, m]$, $f(p_i) = f(p_j) = True$ implies that the values of p_i and p_j are consistently filled or missing across the records from the same key-value node in the template. Additionally, since the list of fields in two key-value blocks generated from the same key-value node are consistent across records, we have $i_{k_1} - j_{k_1} = i_{k_2} - j_{k_2}$. Thus p_i is a perfect match of p_j . When $L_{p_i} > L_{p_j}$, let v'_{p_i} be the subsequence of v_{p_i} that occurs in blocks created from v , i.e., $\forall p_k \in v'_{p_i}, p_k \in B$, where $v \rightarrow B$. Based on the above proof, v'_{p_i} is a perfect match with v_{p_j} , and thus v_{p_i} is a partial perfect match with v_{p_j} . \square

Based on the above propositions, most location vectors are "irregular", while a small amount of them are "regular" (i.e., sharing perfect or partial matches). Informally, regular vectors are fields

Algorithm 1: Field Prediction

```

Input:  $P$ 
1 /*Step 1: Phrase Clustering*/
2  $C \leftarrow \emptyset; P' \leftarrow \text{set}(P)$ 
3 for  $p_i \in P'$  do
4    $\text{merge\_flag} \leftarrow 0$ 
5   for  $C \in C$  do
6     if  $\exists p_j \in C, \text{s.t.}, M(v_{p_i}, v_{p_j}) = 1$  then
7        $C \leftarrow C \cup p_i; \text{merge\_flag} \leftarrow 1$ 
8   if  $\text{merge\_flag} = 0$  then
9      $C \leftarrow \{p_i\}; C \leftarrow C \cup C$ 
10 /*Step 2: Cluster Pruning*/
11  $G \leftarrow (V, E); V \leftarrow C \setminus SL; E \leftarrow \emptyset$ 
12 for  $(C_i, C_j), C_i, C_j \in V$  do
13   if  $\text{Pr}(C_i) > \text{Pr}(C_j)$  and  $w(C_i) < w(C_j)$  then
14      $E \leftarrow E \cup (C_i, C_j)$ 
15  $C_p \leftarrow \text{Maximal}(V)$ 
16 /*Step 3: Cluster Recovery*/
17  $F \leftarrow C_p$ 
18 for  $C_i \in C_p, C_j \in C \setminus C_p$  do
19   if  $\exists p_i \in C_i, p_j \in C_j, L_{p_i} \leq L_{p_j}, \text{s.t.}, \text{PM}(v_{p_i}, v_{p_j}) = 1$  then
20      $F \leftarrow F \cup C_j$ 
21 Return  $F$ 

```

that tend to co-occur together in similar ways (i.e., appear in documents near each other), whereas irregular vectors correspond to values or metadata that occur randomly.

3.1.2 Field Prediction Algorithm. Armed with the above intuition, we outline our field prediction algorithm in Algorithm 1.

Step 1: Phrase Clustering. TWIX first merges any pair of phrases p_i and p_j into one cluster if $M(p_i, p_j) = 1$ (Line 2-9). After clustering, the set of true field phrases per node in the underlying template tend to be in the same cluster, while values tend to be in separate clusters. Consider police complaints in Figure 1. TWIX ensures that the set of true fields appearing in the same table block, such as B_1, B_3 , and B_4 , are merged into one cluster, based on Proposition 1. **Step 2: Cluster Pruning.** The resulting clusters from Step 1 may include many value clusters, which must be pruned. Let $|C|$ denote the number of phrases in cluster C , $\text{Pr}(C)$ the probability that C is a field cluster, and $w(C)$ the width of the confidence interval, respectively. Estimating $\text{Pr}(C)$ requires semantic knowledge to distinguish fields from values, for which LLMs are a promising tool. To estimate $\text{Pr}(C)$, we use LLMs with the prompt: "Given the set of phrases with the type as key or value, return the phrases that are more likely to be keys," appending the phrases in C . $\text{Pr}(C)$ is estimated as the percentage of fields identified by LLMs over all phrases in C . $w(C)$ is computed conditioned on a confidence level 95% as $w(C) = 2 \times 1.96 \times \sqrt{\frac{\text{Pr}(C)(1-\text{Pr}(C))}{|C|}}$. Intuitively, a cluster with high $\text{Pr}(C)$ and small $w(C)$ is likely a field cluster.

We first remove all singletons, denoted as SL , from C (Line 11), as a phrase that does not match with any others is unlikely to be a field. We consider a new graph $G = (V, E)$ on clusters, where $V = C \setminus SL$. We say cluster C_i dominates C_j if $\text{Pr}(C_i) > \text{Pr}(C_j)$ and $w(C_i) < w(C_j)$, implying that C_i has a higher probability to be a field cluster with more confidence than C_j . For any pair of clusters (C_i, C_j) , we add an edge from C_i to C_j if C_i dominates C_j (Line 12-14). Let C_p be the maximal node set of G , where for any cluster $C \in C_p$, there does not exist another cluster $C' \in V$ that dominates C . After the graph is constructed by considering every pair of clusters in V , C_p is returned (Line 15).

Step 3: Cluster Recovery. In Step 2, true field clusters may be pruned if a true field appears in more than one block in a record, resulting in imperfect matches with other true fields. For instance, in the invoice records in Figure 2, the phrase Start Date appears in B_2, B_3 , and B_5 , and is not a perfect match but rather a *partial perfect match* with the other unique true fields in B_2 . This can be shown using Proposition 1, since a sub-sequence of location vectors of Start Date (i.e., occurrences of Start Date in every record) is a perfect match with the location vector of another unique true field (e.g., Line) in B_2 . Here, we recover the clusters including singletons that are partial perfect matches with the identified clusters but weren't identified in previous steps (Line 18-20).

3.2 Row Labeling

Given the set of predicted fields F , TWIX next aims to infer the structure of the template.

3.2.1 Row Label Probabilities and Alignment. Consider the list of phrases P extracted from D , and let $R = [r_1, r_2, \dots]$ be the set of rows in D where r_i represents a list of phrases in a row. Each row $r \in R$ is assigned with one of the four labels, $\{K, V, KV, M\}$, representing *Key*, *Value*, *Key-Value*, and *Metadata*, respectively. For example, r_5, r_8 and r_{10} in Figure 1 are *Key* rows, r_5, r_6, r_9 , and r_{11} are *Value* rows, while r_7 is a *Key-Value* row. In Figure 2, r_9 , starting with Class of Time, is a *Metadata* row.

DEFINITION 3. ROW LABEL PROBABILITIES. Consider a row $r = [p_1, p_2, \dots, p_n]$. Let $\text{Prob}_K^r, \text{Prob}_V^r, \text{Prob}_{KV}^r$ and Prob_M^r be the probability of the row r having the label K, V, KV and *Metadata*, respectively.

$$\text{Prob}_K^r = \frac{1}{m} \sum_{1 \leq i \leq n-1} I(p_i, p_{i+1}, K) \quad (1)$$

$$\text{Prob}_V^r = \frac{1}{m} \sum_{1 \leq i \leq n-1} I(p_i, p_{i+1}, V) \quad (2)$$

$$\text{Prob}_{KV}^r = \frac{1}{m} \sum_{1 \leq i \leq n-1} I(p_i, p_{i+1}, KV) \quad (3)$$

where $m = \sum_{1 \leq i \leq n-1} I(p_i, p_{i+1}, K) + I(p_i, p_{i+1}, V) + I(p_i, p_{i+1}, KV)$

Here I is an indicator function, with $I(p_i, p_{i+1}, K) = 1$ if and only if $p_i \in F$ and $p_{i+1} \in F$, denoting that the pair of phrases (p_i, p_{i+1}) are both fields. Similarly, $I(p_i, p_{i+1}, V) = 1$ and $I(p_i, p_{i+1}, KV) = 1$ denoting that the phrase pair (p_i, p_{i+1}) are both values (i.e., $p_i \notin F$ and $p_{i+1} \notin F$) and a key-value pair (i.e., $p_i \in F$ and $p_{i+1} \notin F$). Additionally, we set $\text{Prob}_M^r = \epsilon$, a small positive number. ($\epsilon = 0.0001$ in our implementation.) We will explain the rationale for this probability shortly. We then normalize the probabilities by dividing each probability $\text{Prob}_x^r, x \in \{K, V, KV, M\}$ by $(1+\epsilon)$. Including ϵ makes a negligible impact on the probability distribution across the labels K, V , and KV as ϵ is very small.

EXAMPLE 4. In Figure 1, consider row r_4 and assume all the phrases in r_4 are predicted as fields. $\text{Prob}_K^{r_4}$ is computed by looking at every consecutive pair of phrases in r_4 , such as (Date, Number), (Number, Investigator), (Investigator, Date Assigned). Since all phrases are predicted as fields, $I(p_i, p_{i+1}, K) = 1$ for all consecutive phrase pairs, and thus $\text{Prob}_K^{r_4} = \frac{1}{1+\epsilon}$, leading to $\text{Prob}_V^{r_4} = 0$ and $\text{Prob}_{KV}^{r_4} = 0$. Consider row r_5 , and assume the phrases Yes

and SUSTAINED are false positives (i.e., they are values but are incorrectly predicted as fields). Then $Prob_V^{r_5} = \frac{3}{5 \times (1+\epsilon)}$, while $Prob_K^{r_5} = \frac{1}{5 \times (1+\epsilon)}$ and $Prob_{KV}^{r_5} = \frac{1}{5 \times (1+\epsilon)}$. Note that the total number of pairs considered in the denominator in r_5 is different from r_4 since there are two missing values and two phrase pairs (p_i, p_{i+1}) where $p_i \notin F$ and $p_{i+1} \in F$ (i.e., label VK), not considered in the label pool. \square

Intuitively, in any label assignment, the set of rows in a true table block should be vertically aligned with its header. In particular, for any value row in a table, it should be visually aligned with its header row. For example, rows r_5 and r_6 should be visually aligned with r_4 in Figure 1. Formally, we define the alignment of two phrases based on their bounding boxes, further define the alignment of two rows.

DEFINITION 4. VERTICAL PHRASE ALIGNMENT. Consider phrases p_i and p_j , with bounding boxes $[x_{i1}, y_{i1}, x_{i2}, y_{i2}]$ and $[x_{j1}, y_{j1}, x_{j2}, y_{j2}]$, respectively. We say p_i and p_j are *vertically aligned*, denoted as $p_i \Vdash p_j$, if $x_{j1} \leq x_{i2} \wedge x_{j2} \geq x_{i1}$.

Just like horizontal alignment $p_i \dashv p_j$, $p_i \Vdash p_j$ is a tolerant notation that allows overlaps. In police record 1 in Figure 1, Date \dashv 5/15/2023 since their bounding boxes overlap vertically, aligning them along a shared vertical axis, while Date $\not\vdash$ 05-01.

DEFINITION 5. ROW ALIGNMENT. Two rows r_i and r_j are *well-aligned*, i.e., $A(r_i, r_j) = 1$, if $\nexists p_{j_k} \in r_j$, s.t., $p_{j_k} \dashv p_{i_1}$ and $p_{j_k} \dashv p_{i_2}$, $p_{i_1}, p_{i_2} \in r_i, i_1 \neq i_2$. Otherwise, $A(r_i, r_j) = 0$.

$A(r_i, r_j) = 1$ simply implies that there does not exist a phrase in a row, say r_i , that overlaps with more than two phrases in the other row r_j . For a Key row r_i and its Value row r_j , r_i and r_j are typically well-aligned, as no field is usually vertically aligned with more than one value in a row. In Figure 1, $A(r_4, r_5) = 1$ since there does not exist a phrase in r_5 that is aligned with two phrases in r_4 . $A(r_4, r_7) = 0$ since Complaint \dashv Date and Complaint \dashv Number. Similarly, $A(r_4, r_8) = 0$ and $A(r_8, r_9) = 1$.

3.2.2 The Row Label Assignment Problem. We now formulate our problem of row label assignment.

DEFINITION 6. ROW LABELING. Consider rows $R = [r_1, r_2, \dots]$, and predicted fields F . We introduce variables y_i^K, y_i^V, y_i^{KV} , and y_i^M for row r_i , where $y_i^K = 1$ implies that r_i has label K; otherwise, $y_i^K = 0$. The problem of template structure inference is as follows:

$$\max \prod_{r_i \in R} (y_i^K Prob_K^{r_i} + y_i^V Prob_V^{r_i} + y_i^{KV} Prob_{KV}^{r_i} + y_i^M Prob_M^{r_i}) \quad (4)$$

$$\text{s.t. : } \forall r_i \in R, y_i^K, y_i^V, y_i^{KV}, y_i^M \in \{0, 1\} \quad (5)$$

$$\forall r_i \in R, y_i^K + y_i^V + y_i^{KV} + y_i^M = 1 \quad (6)$$

$$\forall i, y_i^K \leq \sum_{j>i} A(r_i, r_j) y_j^V \quad (7)$$

$$\forall i, y_i^V \leq \sum_{j<i} A(r_j, r_i) y_j^K \quad (8)$$

The row labeling problem in Definition 6 aims to find the most probable row label assignments by maximizing the products of the probabilities from all rows in R as in (4), under various constraints. Constraints (5) and (6) ensure that each row is assigned exactly one label. Constraint (7) states that for each Key row r_i , there must exist a Value row r_j under r_i ($j > i$) aligned with it ($A(r_i, r_j) = 1$).

Similarly, Constraint (8) says that for each Value row r_j , we expect a Key row r_i before r_j ($i < j$) with $A(r_i, r_j) = 1$, i.e., the values are aligned with keys.

If the *Metadata* label is not introduced, a row r_i could be assigned a label with 0 probability if it violates Constraints (7) and (8). For example, if r_i has $Prob_K^{r_i} = 1$ but lacks a corresponding Value row beneath it, it would be assigned a label with zero probability, leading to a poor assignment. To prevent this, we introduce the *Metadata* label with a low ϵ probability, ensuring the worst possible label for a row is *Metadata*. This adjustment has minimal impact on other rows, as a *Metadata* row does not affect the template structure, such as table or key-value block predictions, nor does it interfere with the assignment of labels with non-zero probability. Empirical observations confirm the effectiveness of the *Metadata* label. True *Metadata* rows are often misclassified as Key rows (e.g., r_3 in police complaints) or Value rows (e.g., r_9 in invoices). Such misclassified rows are typically misaligned with true Key rows, allowing them to be easily identified.

Since the objective in (4) is non-linear, we convert it to be linear below for ease of optimization.

THEOREM 1. The following is equivalent to the objective in Eq. (4),

$$\max_{r_i \in R} \sum (y_i^K \log(Prob_K^{r_i}) + y_i^V \log(Prob_V^{r_i}) + y_i^{KV} \log(Prob_{KV}^{r_i}) + y_i^M \log(Prob_M^{r_i})) \quad (9)$$

PROOF. First, we take log on objective (4), resulting in:

$$\max_{r_i \in R} \sum \log(y_i^K Prob_K^{r_i} + y_i^V Prob_V^{r_i} + y_i^{KV} Prob_{KV}^{r_i} + y_i^M Prob_M^{r_i}) \quad (10)$$

The objective in (10) is equivalent to (4) since logarithms are monotonically increasing. However, this objective is still non-linear. Given the constraint $\forall r_i \in R, y_i^K + y_i^V + y_i^{KV} + y_i^M = 1$, a row r_i can take exactly one label. For simplicity, let $z_i = \log(y_i^K Prob_K^{r_i} + y_i^V Prob_V^{r_i} + y_i^{KV} Prob_{KV}^{r_i} + y_i^M Prob_M^{r_i})$. If $y_i^K = 1$, then all other y_i , such as y_i^V , are 0. In this case, $z_i = y_i^K \log(Prob_K^{r_i})$. Similarly, when $y_i^V = 1$, $z_i = y_i^V \log(Prob_V^{r_i})$. This makes the objective in (10), $\max \sum_{r_i \in R} z_i$, equivalent to the linear objective function in (9). \square

3.2.3 Solving Row Label Assignment: ILP and Hardness. After linearization, the problem defined in Definition 6 with the new objective in (9) is an Integer Linear Programming (ILP) problem. The function $A(\cdot)$ can be precomputed for all row pairs (r_i, r_j) before solving the ILP problem, which makes all the constraints fixed and linear. Note that in the implementation of the above ILP, we additionally add a small $\epsilon = 0.0001$ to the probabilities of all labels to avoid the invalid expression $\log(0)$ in the objective function in (9), and label probabilities are normalized accordingly. This adjustment again does not affect the probability distributions among the different labels for a row as ϵ is small.

THEOREM 2. ROW LABELING IS NP-HARD.

We prove Theorem 2 via a reduction from Minimum Vertex Cover below.

PROOF OF THEOREM 2. We reduce the MINIMUM VERTEX COVER problem to an instance of the row labeling problem. Consider an instance of vertex cover problem, where we are given an undirected graph $G = (V, E)$, with $|V| = n, |E| = m$, and a parameter k . The

decision version of MINIMUM VERTEX COVER asks: Is there a subset $S \subseteq V$, $|S| \leq k$, such that every edge has at least one endpoint in S ?

We now consider an instance of the row labeling problem. We create: $\underbrace{v_1, \dots, v_n}_{\text{vertex rows}} \cup \underbrace{e_1, \dots, e_m}_{\text{edge rows}}$ where each v_i corresponds to

a vertex in V and each e_k corresponds to an edge in E . We index these rows so that $\text{Index}(v_i) = i$ ($i = 1, \dots, n$), $\text{Index}(e_k) = n + k$ ($k = 1, \dots, m$). Hence any vertex row v_i has index $i \leq n$, and any edge row e_k has index $n + k > n$.

We also introduce ‘‘columns’’ of phrases per row to ensure the right alignment across the rows. We have a distinct ‘‘column’’ for each *edge row*. For example, if (a, b) , (a, c) , (b, c) , and (b, d) are edges, we introduce c_{ab} , c_{ac} , c_{bc} , and c_{bd} in some order. Such an order of columns must be consistent across the rows but can be arbitrary. That column aligns with exactly those vertex rows that are the endpoints of that edge (e.g. the column for edge ab aligns only with rows a and b). In matrix terms, this means: $A(a, ab) = 1$, $A(b, ab) = 1$, and $A(x, ab) = 0$ for any other row x .

To ensure this constraint, we introduce text per column. Suppose the columns are indexed $1, 2, 3, \dots, m$. Text phrases for column i begin at α_i and extend until $\alpha_i + \beta$, where α and β are integers greater than 2, and $\alpha > \beta$. The gap between $\alpha_i + \beta$ to $\alpha(i + 1)$ ensures a correct phrase extraction. We then add phrases between α_i and $\alpha_i + \beta$ as follows. For a column corresponding to $e_i = (v_x, v_y)$, that we call c_{v_x, v_y} .

- For edge row e_i , we add a phrase from $[\alpha_i + \beta - 1, \alpha_i + \beta)$.
- For vertex v_x and v_y , we add a phrase from $[\alpha_i, \alpha_i + \beta)$.
- For all other rows, we add a phrase from $[\alpha_i, \alpha_i + \beta - 2]$.

Thus, an edge row $e_i = (v_x, v_y)$ is only aligned with its vertex rows v_x and v_y , and not any other edge or rows. Aggregating information across all rows, we have $A(e, v) = 1$ iff v is one of the endpoints of e . $A(e_i, e_j) = 0, \forall i \neq j$. $A(v_i, v_j) = 1, \forall i \neq j$.

In the following, we will set probabilities such that all edge rows are set as label V , a subset of vertex rows corresponding to a vertex cover will be set as label K , and the remaining vertex rows are set as label KV . In the instance of row labeling problem, each row r_i has four binary variables: $y_i^K, y_i^V, y_i^{KV}, y_i^M$ with $y_i^K + y_i^V + y_i^{KV} + y_i^M = 1$. Constraint 7, $y_i^K \leq \sum_{j>i} A(r_i, r_j) y_j^V$, enforces that if a row is labeled K , it must find a neighbor of higher index labeled V . In our construction, any vertex row v_i (index $i \leq n$) that is K must see some edge row e_k (index $n + k > i$) labeled V for which $A(v_i, e_k) = 1$ (meaning v_i is an endpoint of e_k). Similarly, Constraint 8, $y_i^V \leq \sum_{j<i} A(r_j, r_i) y_j^K$, enforces that if a row is labeled V , it must find a neighbor of lower index labeled K . In our construction, any edge row e_k (index $n + k$) that is V must see some vertex row v_i (index $i < n + k$) labeled K with $A(v_i, e_k) = 1$. So each edge is covered by a K from one of its endpoints.

We now assign *probabilities* for each row+label combination, $Prob_\ell^{r_i}$, where $\ell \in \{K, V, KV, M\}$. We will transform the objective in 9 into a *decision* version by imposing a threshold Θ and asking if $\sum_{r_i \in R} (y_i^K \log(Prob_K^{r_i}) + y_i^V \log(Prob_V^{r_i}) + y_i^{KV} \log(Prob_{KV}^{r_i}) + y_i^M \log(Prob_M^{r_i})) \geq \Theta$. We set $Prob_M^{r_i} = 0$ for any row r_i , hence no solution will assign M to any row. We can change the proof to admit M at a small probability, but we omit it for simplicity. For each edge row e_k , we set $Prob_V^{e_k} = 1$, $Prob_K^{e_k} = 0$, and $Prob_{KV}^{e_k} = 0$. Thus each

edge row is effectively forced to be V . For each vertex row v_i , we set $Prob_K^{v_i} = \lambda$, $Prob_{KV}^{v_i} = \mu$, and $Prob_V^{v_i} = 0$, where $\mu > \lambda$. Hence, labeling v_i as K contributes $\log(\lambda)$ to the sum, while labeling v_i as KV contributes $\log(\mu) > \log(\lambda)$. Thus, if we label x vertices out of n as K , we add $\log(\lambda)x + \log(\mu)(n - x)$. Let k be the parameter in the decision version of the vertex cover problem. Let $\Theta = \log(\lambda)x + \log(\mu)(n - x)$. And therefore the decision version of our row labeling problem becomes $\sum_{r_i \in R} \sum_{\ell \in \{K, V, KV, M\}} y_i^\ell \log(Prob_\ell^{r_i}) \geq \Theta$.

We now show the correctness of the above reduction. On one hand, (\Rightarrow) If G has a vertex cover S , $|S| \leq k$. Label the vertex rows in S as K , the other vertex rows as KV , and all edge rows as V .

- *All alignment constraints are satisfied*: - Each edge row labeled V sees a K neighbor above from among its endpoints in S . - Each K vertex row sees at least one incident edge row V below; otherwise it will not be part of the cover.
- *Total log-prob $\geq \Theta$* : - We used $\leq k$ vertices as K , so $\sum_{r_i \in R} \sum_{\ell \in \{K, V, KV, M\}} y_i^\ell \log(Prob_\ell^{r_i}) \geq \Theta$.

On the other hand, (\Leftarrow) if the row labeling problem meets alignment requirement and the objective is greater than Θ ,

- No row can be labeled M .
- Every edge row is V . Labeling it otherwise means we can improve the objective by changing it to be so.
- At most k vertex rows can be labeled K . If we had more than k vertex rows labeled as K , we will have an objective less than Θ .
- Because each edge row e_k is V , it must see a K neighbor above. So the set of K -labeled vertices forms a valid vertex cover of size $\leq k$.

Hence there is a size- $\leq k$ vertex cover in G if and only if there is a labeling with alignment constraints satisfied and total log-prob $\geq \Theta$. Since MINIMUM VERTEX COVER is NP-complete, deciding whether

$$\max_r \sum_{\ell \in \{K, V, KV, M\}} y_r^\ell \log(Prob_\ell^{r_i}) \geq \Theta$$

is NP-hard. Thus the row labeling problem is also NP-hard. \square

Under the well-known assumption that $NP \neq P$, there does not exist a polynomial-time solution that can solve the problem optimally.

Solving the ILP as stated above can be expensive. Thankfully, inferring the template does not require all of D . Instead, we can use a sublist of rows R containing *at least one record* created from the true template. Let $R' \subseteq R$ be the smallest consecutive sublist of rows in R such that each predicted field $p \in F$ appears at least twice in R' . In TWIX, R' is obtained by scanning rows of R in ascending order and stopping once each predicted field appears twice.

THEOREM 3. Let F' be the true fields in the true template $T' = (V', E')$. If $\exists p \in F \cap F'$, and $\forall Rec, p$ appears exactly once in Rec , then R' contains at least one record Rec created from T' .

Theorem 3 guarantees that if there exists a field p correctly predicted by TWIX, appearing exactly once in every record, then R' contains at least one complete record.

PROOF OF THEOREM 3. If there exist a correctly predicted field $p \in F$ that appears exactly once in every record, and R' contains every field at least twice, then R' contains at least one complete record given that R' is a consecutive sublist of rows. \square

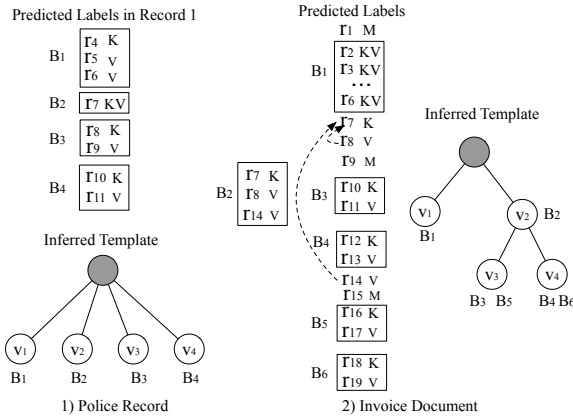


Figure 6: Template Structure Inference.

TWIX considers R' as input to the row labeling problem, and further infers the template in Section 3.3. Empirically, thanks to the small size of input rows $|R'|$ (roughly 32 rows on average in our benchmark), an ILP solver [9] provides a solution in milliseconds. When $|R'|$ is large, we can force the ILP solver to return the best feasible solution so far within the given time limit.

3.3 Template Inference

Given $R' = [r_1, r_2, \dots, r_n]$ with row label predictions, we aim to determine the structure of the underlying template. Let $B = [r_i, r_{i+1}, \dots, r_j]$ be a block consisting of a sequence of rows in D . Let $B.phrases$ be the set of phrases in B .

We begin by initializing an empty template tree $T = (V, E)$ with an artificial root. 1) For every row r_i labeled K , we create a tree node v_i with $v_i.type = table$ and $v_i.fields = r_i$. 2) We merge together as many consecutive rows labeled KV as possible into a block B , and create the corresponding node v_j where $v_j.type = Key-Value$ and $v_j.fields = F \cap B.phrases$. 3) For each row r_i labeled as V , we assign it to its *closest aligned key row* preceding r_i , denoted as r_j , where $j < i$, $r_j.label = K$, $A(r_j, r_i) = 1$, and $\nexists r_k, j < k < i$, such that $r_k.label = K$ and $A(r_k, r_i) = 1$. Note that if a newly created node v_i has the same $v_i.type$ and $v_i.fields$ as an existing node v_j in T , v_i will not be inserted into T . Below, we use two examples to illustrate node creation and tree assembly.

EXAMPLE 5. In Figure 6, the inferred row labels are shown next to the rows. Rows within the same table, such as r_1 and r_2 in Figure 6-1, are aligned and presented together in a block. Rows grouped in the same table block are well-aligned defined in Definition 5 (i.e., each value phrase is vertically aligned with its corresponding field phrase in a table). Consider the police complaints in Figure 6-1. Rows labeled K , specifically r_4, r_8 , and r_{10} , trigger the creation of nodes v_1, v_3 , and v_4 , respectively, while r_7 , labeled KV , corresponds to v_2 . The blocks are sequentially placed with no overlap, with all nodes as leaves. The pre-order traversal of their corresponding nodes in the tree is sorted by block indices (e.g., $ind(B_1) < ind(B_2)$), resulting in the unique template T depicted in Figure 6-1. In the invoice document in Figure 6-2, consecutive KV rows (r_2 to r_6) are merged into a single KV block B_1 . In table block B_2 , r_7 is the closest key row aligned with r_{14} , making r_{14} a value row in B_2 . Note that B_3 and B_5 correspond to the same node v_3 since $r_{17} = v_3.fields$. Therefore, v_3 is created only once, triggered by r_{10} . Because the data block B_2

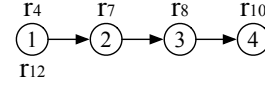


Figure 7: Record Separation in Police Complaints.

(corresponding to v_2) overlaps with B_3 and B_4 (corresponding to v_3 and v_4), v_2 becomes the parent of v_3 and v_4 , while v_1 is a leaf node since its block doesn't overlap with others. \square

Note that sometimes template structure inference can improve field prediction. For example, assume Sustained in r_5 in Figure 1 is incorrectly predicted as a field, and thus a false positive. If the row r_5 is identified as a *Value* row during template inference, the field Sustained is corrected to be a value. The complexity of template inference based on predicted row labels is $O(|R'|^2)$, which is efficient since $|R'|$ is typically small.

4 DATA EXTRACTION

Given the predicted template T and the concatenated document D , TWIX aims to extract data from a set of records $\mathcal{R}ec = [Rec_1, Rec_2, \dots]$ generated by T within D . To do so, we first separate the given document D into records based on T (Section 4.1). Within each record, we further identify the data blocks (Section 4.2), and then extract data from table and key-value blocks (Section 4.3).

4.1 Record Separation

Consider the row representation R of D , $R = [r_1, r_2, \dots]$. Recall that a block B is a sequence of rows. For any node $v \in V$ in the template T , we say that node v is *visited* by block B if all the fields of v appear in block B , i.e., $v.fields \subseteq B.phrases$, denoted by $vis(v, B) = True$. Intuitively, a record is the smallest block that visits *every* node in T *at least once* via a *pre-order* traversal. The document D is now separated into a list of records $\mathcal{R}ec$.

EXAMPLE 6. Given the predicted template T as shown in Figure 4-1, we aim to separate records 1 and 2 in Figure 1. We scan each row $r_i \in D$ in ascending order of index, and consider the pre-order traversal of nodes in T in Figure 7. $vis(v_1, [r_4])$ is True as $v_1.fields = r_4$ (r_4 is the header of the table block corresponding to v_1), and v_1 is thus visited. Similarly, $[r_7]$ visits v_2 as $v_2.fields \subseteq r_7$, and $[r_{10}]$ visits v_4 . When r_{12} visits v_1 the second time ($v_1.fields = r_{12}$), all nodes in T have been visited at least once, and v_1 being visited by r_{12} the second time implies the start of a new record. Note that it is not necessary that each node is visited exactly once, because nested nodes (e.g., v_3 in invoice template) may be visited multiple times. \square

4.2 Block Separation

Given a record $Rec \in \mathcal{R}ec$ from the previous step, we aim to identify a list of blocks corresponding to each node in T within D . For instance, Figures 1 and 2 exemplify the data blocks within a record in police complaints and invoices, respectively.

Block separation proceeds in two steps as in Algorithm 2. First, we assign the labels for each row $r \in Rec$ based on the template T . Given a row $r = [p_i, \dots, p_j]$, if $\exists v \in V, v.type = Table, \forall p \in v.fields, p \in r$, then $r.label = K$ (Lines 2-4). Otherwise, if $\exists v \in V, v.type = Key-Value, r \cap v.field \neq \emptyset, r.label = KV$ (Lines 5-6). In all the other cases, $r.label = V$ (Lines 7-8). A row with label V might be corrected to be a *Metadata* row, as shown next. Second, for a value row r_i whose label is V , let r_j be the closest key row preceding

Algorithm 2: Block_Separation($Rec, T = (V, E)$)

```

1 /*Step 1: Row Label Assignment*/
2 for  $r \in Rec$  do
3   if  $\exists v \in V, v.type = table, v.fields = r$  then
4      $r.label = K$ 
5   else if  $\exists v \in V, v.type = key-value, r \cap v.field \neq \emptyset$  then
6      $r.label = KV$ 
7   else
8      $r.label = V$ 
9 /*Step 2: Block Separation*/
10 Member  $\leftarrow \emptyset$ 
11 for  $r_i \in Rec, r_i.label = V$  do
12    $r_j \leftarrow \text{closest\_preceding\_key\_row}(r_i)$ 
13   if  $A(r_i, r_j) = 1$  then
14     Member( $r_j$ ).append( $r_i$ )
15   else
16      $r_l \leftarrow \text{closest\_preceding\_aligned\_key\_row}(r_i)$ 
17     if  $\exists r_l, v_l, hasChild = True$  then
18       Member( $r_l$ ).append( $r_i$ )
19     else
20        $r_i.label = Metadata$ 
21 for  $r_i, r_{i+1} \in Rec$  do
22   if  $r_i.label = KV$  and  $r_{i+1}.label = KV$  then
23     Member( $r_i$ ).append( $r_{i+1}$ )
24 Return Member

```

r_i . If r_i is aligned with r_j , i.e., $A(r_j, r_i) = 1$, then r_i is assigned to be a value row of the table with the key row as r_j (Lines 11-14). Otherwise, if there exists another key row r_l preceding and as close as possible to r_i , where $A(r_l, r_i) = 1$ and the corresponding node v is not a leaf, r_i is assigned to be a value row of r_l (Lines 15-18). In other cases, r_i is labeled as *Metadata* (Lines 19-20), as it is neither aligned with any K row (and thus not a valid V row) nor predicted to be a KV or K row. Finally, for any consecutive key-value rows, we merge them together into one block (Lines 21-23).

EXAMPLE 7. Consider the police complaints in Figure 1 and its predicted template in Figure 4-1. The labels for r_4, r_8 , and r_{10} are K , r_7 's label is KV , and all other rows are labeled V . Row r_5 is assigned to r_4 because r_4 is aligned with r_5 and is the closest preceding key row. Similarly, r_9 is assigned to r_8 . Now consider the invoice document in Figure 2 and its predicted template in Figure 4-2. The closest preceding key row to r_{14} is r_{12} . However, r_{12} is not the key row for r_{14} because they are not aligned. The closest preceding key row aligned with r_{14} is r_7 , corresponding to node v_2 in the template. Since v_2 is not a leaf node, its data block can overlap with others as defined in Section 2. Thus, r_{14} is correctly assigned to r_7 . \square

Each record $Rec \in \mathcal{R}ec$ now is transformed into a list of data blocks, either table or key-value blocks.

4.3 Data Extraction

Data is then extracted differently for table and key-value blocks.

Data Extraction in Table Block. Given a table block B , we next extract its contents. Let $B.fields = [f_1, f_2, \dots, f_n]$ be the list of predicted fields in B sorted in ascending order of index.

The first row r_l in B corresponds to $B.fields$, and each value row $r_i \in B, r_i \neq r_l$ corresponds to a tuple of this table, where $r_i = [p_{i1}, p_{i2}, \dots, p_{im}]$. Intuitively, the values corresponding to a field are typically aligned vertically as a column in a table block. Thus, given a value row $r_i \in B$, if p_{ij} is vertically aligned with f_j , i.e., $p_{ij} \vDash f_j$, then p_{ij} is determined to be a value of f_j . Given a field f_j , if there does not exist a value $p_{ij} \in r$, such that $p_{ij} \vDash f_j$, then f_j 's value is missing (or NULL) for row r_i . Consider data extraction of

Algorithm 3: KV-Extract(B)

```

1 seen  $\leftarrow \{\}$ ;  $i \leftarrow 0$ ;  $KV \leftarrow \emptyset$ 
2 for  $p_i \in B$  do
3    $seen[i] \leftarrow False$ 
4 while  $i < |B| - 1$  do
5   if  $seen[i] == False$  then
6     if  $p_i \in B.fields \wedge p_{i+1} \notin B.fields$  then
7        $KV \leftarrow KV \cup (p_i, p_{i+1})$ 
8        $seen[i+1] \leftarrow True$ 
9     if  $p_i \in B.fields \wedge p_{i+1} \in B.fields$  then
10       $KV \leftarrow KV \cup (p_i, missing)$ 
11     $i \leftarrow i + 1$ 
12 Return  $KV$ 

```

block B_1 in Record 1 for police complaints in Figure 1. The value for Completed is missing in r_5 , 05-01 and Yes are the values for Number and Recorded On Camera in r_5 , respectively.

Data Extraction in Key-Value Block. In a key-value block B , a field either has a corresponding value or may be missing. In Algorithm 3, to extract key-value pairs given predicted fields, we sequentially scan each consecutive phrase pair (p_i, p_{i+1}) in B . We use an array $seen[i]$ to track whether the phrase p_i has been scanned. If (p_i, p_{i+1}) forms a key-value pair, i.e., $p_i \in B.fields \wedge p_{i+1} \notin B.fields$, it is added to the extraction result (Lines 6-7). We then examine the next phrase pair starting from p_{i+2} by setting $seen[i+1]$ to True. If both phrases are fields, the phrase p_i is assigned a missing value, and we proceed by examining the phrase pair starting with p_{i+1} (Lines 9-10). For example, if Complaint and DOB in row r_7 in Figure 1 are identified as fields, their values are predicted as missing.

Encode Extraction Results. Finally, after extracting data from the data blocks in each record, we assemble the results into a tree. Let o_i denote the *data extraction object* of a data block B_i , associated with three attributes: $o_i.fields$, $o_i.type$, and $o_i.content$. Here, $o_i.fields = B_i.fields$, and $o_i.type \in \{Table, Key-Value\}$ based on the type of B_i . When $o_i.type = Key-Value$, $o_i.content$ is a list of key-value pairs. When $o_i.type = Table$, $o_i.content$ represents the extracted table, with $o_i.fields$ as the header and the corresponding extracted tuples.

Let O be the *data extraction object* of a record Rec , and O is a tree, where the nodes are the set of data extraction objects of blocks in Rec . For two nodes o_i, o_j , if o_i is a parent of o_j , then $B_i \cap B_j \neq \emptyset$ and $ind(B_i) < ind(B_j)$, i.e., B_i appears before B_j and B_i overlaps with B_j . If o_i is a left sibling of o_j , then $B_i \cap B_j = \emptyset$ and $ind(B_i) < ind(B_j)$.

EXAMPLE 8. The data extraction objects of the first record for police complaints and invoices are presented in Figure 8. For Rec_1 in police complaints, four data extraction objects o_1, o_2, o_3 and o_4 are sequentially placed under the root, while in invoices, o_2 is the parent of o_3 as their blocks B_2 and B_3 overlaps and B_2 appears before B_3 in Figure 2. \square

In addition to returning the data extraction objects, TWIX stores metadata and preserves their associations with the data extraction objects. To achieve this, TWIX stores the bounding box and page number for every metadata phrase. In police complaints in Figure 1, if r_1, r_2 , and r_3 are predicted as metadata rows, their bounding boxes and page numbers reveal that these metadata are located above the first data extraction object, likely serving as the header of the document. As another example, the metadata phrase Complaints # 1 in row r_9 is located in the same row as the first extracted tuple in the table block B_3 , based on stored bounding boxes. Users can leverage this information to perform data transformations, such

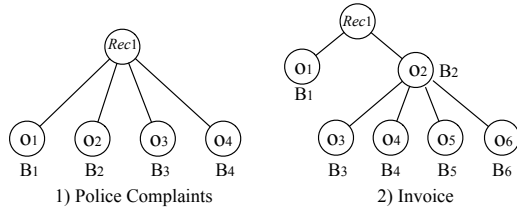


Figure 8: Data Extraction Objects of the First Record for Police Complaints and Invoices.

as augmenting the extracted data in B_3 by creating a new column called `Complaint` and populating its value as 1 in the first row. Since data transformations depend on user needs and preferences, we leave the task of transforming metadata to enrich the data object to the end users, which is beyond the scope of our work.

4.4 Analysis

Now we analyze the correctness of the returned data extraction objects in one commonly observed type of document that we call *compliant documents*, defined below.

DEFINITION 7. COMPLIANT DOCUMENT. Consider a table block B . If every value phrase is uniquely vertically aligned with its field phrase, then B is a *compliant table block*. Consider a key-value block $B = [p_1, p_2, \dots, p_m]$, where p_i is a phrase. If $\forall p_i \in B, p_i \notin B.fields$, we have $p_{i-1} \in B.fields$, then B is a *compliant key-value block*. Given a document D , if $\forall B \in D, B$ is compliant, then D is a *compliant document*.

In a compliant table block, every value row is vertically aligned with the header row in the table, while in a compliant key-value block B , every value $p \notin B.fields$ has a preceding field.

THEOREM 4. For a compliant document D whose Metadata rows are not well-aligned with any Key rows, the data extraction objects for D are correct as long as the phrases P in D are extracted correctly and the prediction of T is correct.

Many real-world templated documents in our benchmark are complex due to intricate template structures. However, most individual data blocks—whether table or key-value blocks—are compliant. Across 34 real-world datasets with over 1,000 documents spanning diverse domains, 91% of the documents are compliant. For the non-compliant cases, removing just 3% of non-compliant phrases results in compliant documents. A non-compliant phrase refers to a table cell misaligned with its field or a value in a key-value block without a corresponding field. Thus, Theorem 4 provides correctness guarantees for our approach across extensive real-world datasets, with a detailed proof below. At the end of Section 5, we present an empirical analysis of scenarios where TWIX fails.

PROOF OF THEOREM 4. If the prediction of T is correct, then the set of fields is accurately predicted for each data block. Any metadata row r not aligned with a key row will be correctly identified as metadata in Algorithm 2. Furthermore, data block separation is correct if the predicted template T matches the true template, as all records are generated using the same T . In a compliant table block, TWIX correctly extracts all field-value mappings in the key row and its value rows since each value phrase is uniquely vertically aligned with its corresponding field phrase. Similarly, TWIX accurately extracts key-value pairs in a compliant key-value block because every true value has a preceding key. This concludes the proof. \square

	# of Datasets	Avg Dataset Size (tokens)	Avg # of Doc
Easy	6	5902	11.2
Medium	21	7813	6.8
Hard	7	6417	5.1

Table 1: Characteristics of 34 Datasets.

5 EXPERIMENTAL EVALUATION

We evaluate the performance of our approaches on data extraction over 34 real-world templated documents.

5.1 Evaluation Setup

Datasets. We collected 34 real-world datasets from our journalism collaborators, and three open benchmarks [35, 44, 49], spanning diverse domains such as police use of force documents, invoices, grant reports, order bills, certification records, contracts, and trade forms. We randomly sampled 5 to 30 documents per dataset, based on the dataset size, with fewer samples for smaller datasets and more for larger ones to ensure representative coverage.

We classify the 34 datasets into three types based on complexity: Easy, Medium, and Hard. Easy datasets have templates with only one node besides the virtual root, meaning the document is either a pure table block or a key-value block. For simplicity, we omit the virtual root when discussing nodes in templates. Medium datasets feature templates with more than two nodes, all in the same layer (i.e., all nodes are leaves), indicating sequentially placed, non-overlapping data blocks within a record (e.g., police complaints). Hard datasets have nodes with children, implying overlapping data blocks, as in invoices in Figure 2. Table 1 summarizes the dataset characteristics, including the number of datasets per type, average size, and average number of documents per dataset. The ground truth for all datasets was manually collected and verified by three human labelers over a month, highlighting the task’s complexity even for humans.

Tools Compared. We compare TWIX with four baselines. This includes Amazon *TextExtract* [1], and Azure AI Document Intelligence (*AzureDI* for short) [2], which detect and extract tables and key-value pairs from PDFs. We also include two state-of-the-art vision-based LLMs, *vLLM-S* and *vLLM-C*, both using *gpt4vision* [6] from OpenAI. *vLLM-S* uses a prompt to identify the template structure and extract data, while *vLLM-C* focuses on extracting all key-value pairs from a given document. For a table, *vLLM-C* extracts each cell and its header as key-value pairs, whereas for key-value blocks, it outputs a list of key-value pairs. Prompts for *vLLM-S* and *vLLM-C* is shown below. We also considered using text-based LLMs, which takes the OCR output from a PDF and then performs data extraction. As both vision-based LLMs outperform any text-based LLMs we tried, we omit it in our result.

Metrics. We report precision and recall to evaluate the quality of the extracted results. For TWIX, if an extracted object is a table, we convert it to a list of key-value pairs for each cell with its corresponding key in the header. If a cell contains a missing value, we include *(key, missing)* as part of the output. Key-value blocks naturally represent key-value pairs. We similarly transform the extracted results from the baselines into a list of key-value pairs as the extraction result for each document per dataset. For a document D , let KV_p and KV_t be the predicted key-value pairs and true key-value pairs for D . Precision $P_D = \frac{|KV_p \cap KV_t|}{|KV_p|}$, while recall $R_D = \frac{|KV_p \cap KV_t|}{|KV_t|}$. For a dataset $\mathcal{D} = \{D_1, D_2, \dots\}$, $P_{\mathcal{D}}$ and $R_{\mathcal{D}}$ represent

	Precision					Recall				
	Textract	vLLM-S	vLLM-C	AzureDI	TWIX	Textract	vLLM-S	vLLM-C	AzureDI	TWIX
Easy	0.9	0.74	0.73	0.54	0.98	0.88	0.62	0.68	0.68	0.97
Medium	0.5	0.63	0.6	0.49	0.88	0.51	0.57	0.5	0.62	0.9
Hard	0.38	0.59	0.64	0.35	0.85	0.44	0.49	0.57	0.66	0.88

Table 2: Precision and Recall on Easy, Medium and Hard Datasets.

the average precision and recall over documents in \mathcal{D} . We report average precision and recall on Easy, Medium, and Hard datasets.

```

Prompt of vLLM-S:
Please extract all key-value pairs from the
following image and output only the same JSON
template below. For key-value blocks, extract
the pairs directly. For tables, output a key-
value pair for every cell using the table
headers as keys. Do not attempt to interpret
the overall structure; simply extract and
present all key-value pairs as they appear.
JSON Template:
[
  {
    "content": [
      {
        "type": "table",
        "content": [
          {
            "key1": "value1",
            "key2": "value2"
          },
          {
            "key1": "value3",
            "key2": "value4"
          },
          ... more key-value pairs ...
        ]
      },
      {
        "type": "kv",
        "content": [
          {
            "key1": "value1"
          },
          ... more key-value pairs ...
        ]
      }
    ]
  }
]

```

```

Prompt of vLLM-C:
Please extract ALL key-value pairs from the
following image and output only the same JSON
template below. For key-value blocks, extract
the pairs directly. For tables, output a key-
value pair for every cell using the table
headers as keys. Do not attempt to interpret
the overall structure; simply extract and
present all key-value pairs as they appear.
JSON Template:
{
  "key1" : "value1",
  "key2" : "value2",
}

```

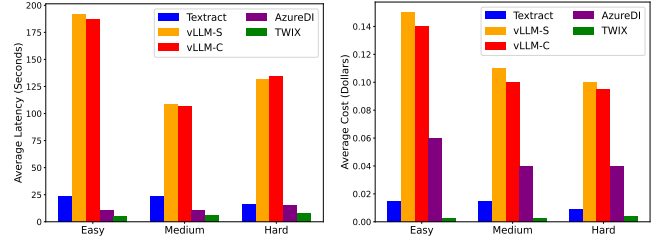


Figure 9: Latency Comparisons. Figure 10: Cost Comparisons.

5.2 Experimental Results

Experiment 1: Quality Comparisons. We report the precision and recall for all tools in Table 2. In Easy datasets, both Textract and TWIX perform well, with *TWIX outperforming Textract by around 8% in precision and 9% in recall*. Vision-based LLM approaches and AzureDI struggle even on simple templates. A common error pattern is that when there are multiple consecutive missing values in a row of a table, vision-LLMs often fail to detect the exact number of consecutive missing values, causing misalignment between the extracted cells and their corresponding keys. AzureDI fails to correctly identify the table header in some datasets, leading to quality degradation.

TWIX significantly outperforms the baselines in both Medium and Hard datasets, achieving around *38% higher precision and 39% higher recall compared to Textract, 44% higher precision and 25% higher recall compared to AzureDI, and 25% higher precision and 33% higher recall compared to the best vision-LLM approach*. All baselines struggle with complex layouts, leading to a significant drop in quality. This highlights the importance of recovering the template first, which makes downstream data extraction more accurate, compared to general-purpose data extraction solutions that ignore the underlying template.

Experiment 2: Latency Comparisons. We compare the end-to-end latency in Figure 9. Vision LLM approaches are time-consuming, as they process each page as an image. Their latency depends on the number of pages and the size of the output tokens. Data extraction tasks typically return a large number of output tokens, making image-based extraction costly. Textract and AzureDI are much faster than vLLM-based baselines, taking around 21 and 11s to extract data for documents with an average of 10.4 pages per dataset, respectively. TWIX is the most efficient tool, taking around 5s to process a dataset—*2× faster than AzureDI, 4× faster than Textract, and 28.6× faster than vLLM-based approaches*.

Experiment 3: Cost Comparisons. Figure 10 presents the end-to-end cost of all tools. All baselines charge per page. Textract and AzureDI have fixed rates of \$1.50 and \$100 per 1000 pages, respectively [1, 2], while GPT-4-Vision APIs charge based on the number of pages and image resolution (treating each page as an image) [7]. TWIX incurs costs only during template prediction, where LLMs filter non-field phrase clusters. The subsequent template-based extraction is LLM-free, incurring no further cost. Across all datasets,

	Data	OCR	Template Prediction	Data Extraction
Latency	Easy	15.7%	82.4%	1.9%
	Medium	12.8%	85.5%	1.7%
	Hard	11.9%	86.4%	1.7%
	Large	75.1%	21.7%	3.2%
Cost	Easy	0%	100%	0%
	Medium	0%	100%	0%
	Hard	0%	100%	0%
	Large	0%	100%	0%

Table 3: Breakdown of Latency and Cost of TWIX.

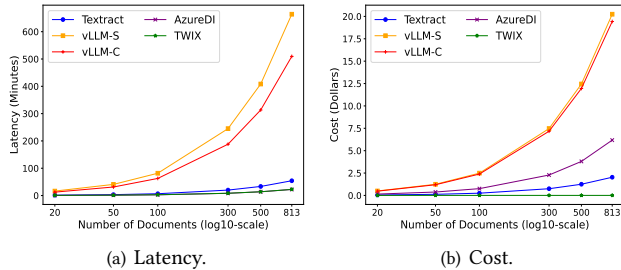


Figure 11: Scalability Evaluation on a Large Dataset.

TWIX achieves an average cost of less than \$0.003 per dataset, representing 23% of Textract’s cost, 6.4% of AzureDI’s cost, and 0.8% of vision-LLM-based tools’ cost.

Experiment 4: Scalability Comparisons. To evaluate how the tools scale to large datasets, we selected Active_Employment, the largest dataset, containing 813 documents created using the same template, each with one page.

Figure 11 illustrates the cost and latency of all tools, with the x-axis on log scale. TWIX can scale to large datasets easily thanks to template prediction. TWIX first learns the template from the first few documents, then extracts data for remaining documents based on the predicted template without invoking LLMs, resulting in highly efficient extraction at a low cost. TWIX incurs no additional cost as the number of documents grows and introduces negligible latency since template-based data extraction is inexpensive.

This demonstrates the crucial role of template prediction for data extraction on templated documents, which explains TWIX’s performance advantage over the baselines in latency, cost, and accuracy. Conversely, all baselines’ latency and cost increase linearly with the number of documents. Vision-based LLMs, for example, take over 10 hours to process 813 pages at approximately \$20. **TWIX completes the task in 53.1 seconds—734× faster and 5836× cheaper (0.018% of the cost) than the vision-LLM based solution.**

Experiment 5: Time and cost breakdown of TWIX. TWIX consists of three components: 1) extracting plain text from PDF documents using OCR tools; 2) template prediction, where TWIX predicts the set of fields and the structure of the template; and 3) data extraction using the predicted template. We provide a breakdown of latency and cost for these three components in Table 3. This evaluation is conducted on the Easy, Medium, and Hard datasets, as well as the large dataset used in Experiment 4. The numbers represent the percentage of latency and cost for each component.

All costs from TWIX are incurred during the template prediction stage, particularly in predicting the fields where LLMs are involved. When the dataset size is relatively small, as in the Easy, Medium, and Hard datasets, template prediction consumes around 85% of the time, and data extraction is the fastest component. However,

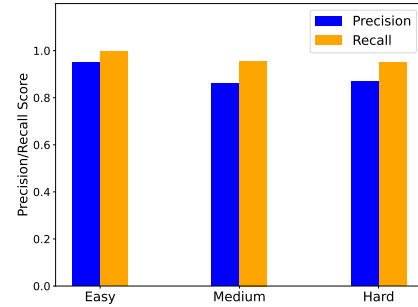


Figure 12: Performance of Field Prediction.

as the dataset size grows, the most time-consuming component becomes OCR, as its time increases linearly with the number of documents, while template prediction is a one-time process and remains constant regardless of dataset size.

Experiment 6: Performance of Field Prediction. We examine the performance of the field prediction in TWIX, described in Section 3.1, and report precision and recall in Figure 12.

In Easy datasets with simple template structures, the precision and recall of the set of predicted fields are around 0.95 and 0.98, respectively. When the template becomes more complex, as in the Medium and Hard datasets, the precision drops to around 0.86 while the recall still remains close to 0.95. A high recall is important for predicting the template structure since the set of key rows will likely be recovered, which are the backbone of table blocks.

Template structure prediction helps correct field prediction errors. First, metadata (headers, footers, etc.) incorrectly predicted as keys/values are often corrected, as they rarely align with rows in table or key-value blocks, violating constraints in the row labeling problem. Second, false positives are frequently corrected after row labeling. For instance, the false positives in a value row will be corrected once the row is identified as a value row. These observations highlight TWIX’s robustness in field prediction.

Experiment 7: Error Pattern Analysis. We identify six common error types observed in the compared tools below and summarize them in Table 4, where we use ✓✓ and ✓ to indicate errors that most significantly affect and moderately affect each tool, respectively. Note that all tools exhibit some degree of error in every type. For errors that have minimal impact on a tool’s performance, no corresponding check mark is included in the table.

Type (1): Column Misalignment. When multiple consecutive values are missing in a row in a table block, vision LLM approaches often fail to count the exact number of missing values, resulting in mismatched values and rows. **Type (2): Misidentification of Table Headers.** AzureDI fails to identify the table header correctly, instead selecting the first row as the header in 4 out of 34 datasets. Textract similarly misidentifies table headers, particularly in documents with complex layouts. **Type (3): Misidentification of Data Blocks.** All baselines struggle to accurately identify data blocks in complex layouts, such as in Medium and Hard datasets. They may miss data blocks entirely or merge multiple blocks into one. For example, vision-based LLMs show inconsistent behavior, occasionally extracting partial data or missing entire blocks. **Type (4): Phrase Extraction Errors from OCR.** OCR-based Phrase extraction is imperfect and affects all tools. OCR may merge closely spaced phrases into one or split a long phrase into multiple parts. While such errors are relatively infrequent, they can still impact results, particularly when fields like table headers are extracted incorrectly.

	Type 1	Type 2	Type 3	Type 4	Type 5	Type 6
Texttract		✓✓	✓✓	✓	✓	✓✓
vLLM-S	✓✓		✓✓	✓	✓	✓✓
vLLM-C	✓✓		✓✓	✓	✓	✓
AzureDI		✓✓	✓✓	✓	✓	✓✓
TWIX				✓	✓	✓✓

Table 4: Frequent Error Patterns of Compared Tools.

Type (5): Metadata Misclassified as Fields or Values. If a metadata row is misclassified as a value row and aligns with a table header, TWIX incorrectly includes it in the table block, causing false positives. Similar behavior is observed in other tools; vision-LLMs frequently create new fields for metadata and incorporate them into data blocks. **Type (6): Field Prediction Errors.** None of the tools achieve perfect field prediction, which affects downstream tasks such as table or key-value block prediction in the baselines or row labeling in TWIX.

6 RELATED WORK

Our work is relevant to document and web data extraction, as well as document layout analysis.

Document Data Extraction. There have been multiple papers [10, 43, 47] and industrial tools [1, 3, 4] aimed at extracting data from documents. Most extraction tools, e.g., [1, 3, 4, 10, 43] are general-purpose solutions for extracting tables or entities from visually rich form-like documents.

Tools from industry like Texttract [1], Google Document AI [4], and Azure Document Intelligence [3] use pretrained models to extract structured data, such as tables or key-value pairs, from form-like documents. These tools perform well on simple layouts and domains well-represented in their training data (e.g., Google Document AI offers models for specific domains like taxes or invoices). However, they often fail on unseen documents with complex layouts and incur significant costs and latency. Recent advances in vision-based LLMs, such as GPT-4 Vision [6], show promise but lack consistent performance, with high latency and substantial costs, as demonstrated in our experiments.

Learning-based extraction [13, 29, 31, 34, 37, 38, 47, 51] retrieves values for user-specified fields from documents by training deep learning models on human-labeled data. However, it requires significant human effort (e.g., specifying fields and labels) and doesn’t capture relationships between extracted field values, as discussed in Section 1. In contrast, our unsupervised approach uncovers the template—the backbone of templated documents—and efficiently extracts structured data. For example, Parthasarathy et al. [40] introduce the concept of landmarks to narrow down the region of interest in a document and then extract values for user-specified fields, while TWIX preserves relationships in the extracted data.

Web Data Extraction. Our work is also related to web data extraction, which primarily relies on HTML tags [11, 12, 15, 18, 20, 22–27, 30, 32, 36, 39, 42, 43]. The earliest work in this vein analyzed differences between pages generated using the same HTML template to learn the template through techniques like regular expressions [12, 22, 30, 32]. Other papers extended this to develop robust wrappers to handle the evolution of underlying HTML templates in web pages over time [23, 39], while others explored generating domain-centric wrappers for web-scale information extraction, designed to tolerate noise [15, 24–26]. For example, Miria [20] extracts records from websites by identifying invariants across records based on HTML tag trees. Cetorelli et al. [18] introduce a

landmark-based grammar from a set of web pages with a common HTML template. To extract relations from semi-structured web data, Lockard et al. [43] proposed a distant supervision approach, while DeepDive [36] further leveraged XML and HTML-specific feature descriptors. However, HTML or XML tags present in web-pages or semistructured documents indicating nesting relationships are often not available in documents like PDFs.

Several studies extract tables from the web without relying on HTML tags. Chu et al. [21] split phrases in record rows into cells aligned with corresponding columns, while Chen et al. [19] extract information from spreadsheets by leveraging font formatting to extract metadata and using learning-based methods to label rows. Cafarella et al. [17] extract fact tuples by parsing natural language sentences on the web. Finally, Gao et al. [28] explore an unsupervised approach to extract structures for log datasets. These methods primarily focus on data with simple layouts or structures, like tables or logs, whereas our approach handles complex visual layouts, including nested combinations of tables and key-value structures. **Document Layout Analysis.** Document layout analysis (DLA) [14, 16, 33, 41, 45, 46, 48, 50] detects various document layouts, such as pages, texts, tables, images, titles, headers, and footers, using visual features (e.g., font size and type), content, and structural patterns. While effective for coarse-grained components like text and table blocks, DLA struggles with fine-grained components, such as mixed key-value and table blocks. Combining DLA with our approach could potentially enhance data extraction by first detecting structured portions in long documents with text or images, allowing our method to handle the structured parts and expanding its applicability. This remains an interesting avenue for future work.

7 CONCLUSION

We present TWIX, a robust, efficient, and effective tool to extract structured data from a collection of templated documents. TWIX first infers a flexible visual template used to create documents, using which it separates templated documents into nested records and data blocks within records, enabling accurate and efficient data extraction from each block. We demonstrate hardness for the underlying problems, while also providing correctness guarantees. TWIX combines an optimization approach for principled template discovery, while leveraging LLMs to provide semantic knowledge in carefully targeted ways. Our experiments show that TWIX outperforms baselines significantly across accuracy, latency, and cost.

REFERENCES

- [1] 2024. <https://aws.amazon.com/textract/>.
- [2] 2024. <https://azure.microsoft.com/en-us/products/ai-services/ai-document-intelligence>.
- [3] 2024. <https://azure.microsoft.com/en-us/products/ai-services/ai-document-intelligence>.
- [4] 2024. <https://cloud.google.com/document-ai>.
- [5] 2024. <https://github.com/jsvine/pdfplumber>.
- [6] 2024. <https://help.openai.com/en/articles/8555496-gpt-4-vision-api>.
- [7] 2024. <https://openai.com/api/pricing/>.
- [8] 2024. <https://pymupdf.readthedocs.io/en/latest/>.
- [9] 2024. <https://www.gurobi.com/resources/ch4-linear-programming-with-python/>.
- [10] Milan Aggarwal, Himesh Gupta, Mausoom Sarkar, and Balaji Krishnamurthy. 2021. Form2Seq: A framework for higher-order form structure extraction. *arXiv preprint arXiv:2107.04419* (2021).
- [11] Eugene Agichtein and Luis Gravano. 2000. Snowball: Extracting relations from large plain-text collections. In *Proceedings of the fifth ACM conference on Digital libraries*. 85–94.
- [12] Arvind Arasu and Hector Garcia-Molina. 2003. Extracting structured data from web pages. In *Proceedings of the 2003 ACM SIGMOD international conference on Management of data*. 337–348.
- [13] Ting Bai, Ji-Rong Wen, Jun Zhang, and Wayne Xin Zhao. 2017. A neural collaborative filtering model with interaction-based neighborhood. In *Proceedings of the 2017 ACM on Conference on Information and Knowledge Management*. 1979–1982.
- [14] Galal M Binnmakhashen and Sabri A Mahmoud. 2019. Document layout analysis: a comprehensive survey. *ACM Computing Surveys (CSUR)* 52, 6 (2019), 1–36.
- [15] Philip Bohannon, Nilesh Dalvi, Yuval Filmus, Nori Jacoby, Sathya Keerthi, and Alok Kirpal. 2012. Automatic web-scale information extraction. In *Proceedings of the 2012 ACM SIGMOD International Conference on Management of Data*. 609–612.
- [16] Thomas M Breuel. 2003. High performance document layout analysis. In *Proceedings of the Symposium on Document Image Understanding Technology*, Vol. 5.
- [17] Michael J Cafarella, Jayant Madhavan, and Alon Halevy. 2009. Web-scale extraction of structured data. *Acem Sigmod Record* 37, 4 (2009), 55–61.
- [18] Valerio Cetoirelli, Paolo Atzeni, Valter Crescenzi, and Franco Milicchio. 2021. The smallest extraction problem. *Proceedings of the VLDB Endowment* 14, 11 (2021), 2445–2458.
- [19] Zhe Chen and Michael Cafarella. 2013. Automatic web spreadsheet data extraction. In *Proceedings of the 3rd International Workshop on Semantic Search over the Web*. 1–8.
- [20] Zhijia Chen, Weiyi Meng, and Eduard Dragut. 2022. Web record extraction with Invariants. *Proceedings of the VLDB Endowment* 16, 4 (2022), 959–972.
- [21] Xu Chu, Yeye He, Kaushik Chakrabarti, and Kris Ganjam. 2015. Tegra: Table extraction by global record alignment. In *Proceedings of the 2015 ACM SIGMOD international conference on management of data*. 1713–1728.
- [22] Valter Crescenzi and Giansalvatore Mecca. 2004. Automatic information extraction from large websites. *Journal of the ACM (JACM)* 51, 5 (2004), 731–779.
- [23] Nilesh Dalvi, Philip Bohannon, and Fei Sha. 2009. Robust web extraction: an approach based on a probabilistic tree-edit model. In *Proceedings of the 2009 ACM SIGMOD International Conference on Management of data*. 335–348.
- [24] Nilesh Dalvi, Ravi Kumar, Bo Pang, Raghu Ramakrishnan, Andrew Tomkins, Philip Bohannon, Sathya Keerthi, and Srujana Merugu. 2009. A web of concepts. In *Proceedings of the twenty-eighth ACM SIGMOD-SIGACT-SIGART symposium on Principles of database systems*. 1–12.
- [25] Nilesh Dalvi, Ravi Kumar, and Mohamed Soliman. 2011. Automatic wrappers for large scale web extraction. *arXiv preprint arXiv:1103.2406* (2011).
- [26] Nilesh Dalvi, Ashwin Machanavajjhala, and Bo Pang. 2012. An analysis of structured data on the web. *arXiv preprint arXiv:1203.6406* (2012).
- [27] Oren Etzioni, Michael Cafarella, Doug Downey, Stanley Kok, Ana-Maria Popescu, Tal Shaked, Stephen Soderland, Daniel S Weld, and Alexander Yates. 2004. Web-scale information extraction in knowitall: (preliminary results). In *Proceedings of the 13th international conference on World Wide Web*. 100–110.
- [28] Yihan Gao, Silu Huang, and Aditya Parameswaran. 2018. Navigating the data lake with datamaran: Automatically extracting structure from log datasets. In *Proceedings of the 2018 International Conference on Management of Data*. 943–958.
- [29] Anoop Raveendra Katti, Christian Reisswig, Cordula Guder, Sebastian Brarda, Steffen Bickel, Johannes Höhne, and Jean Baptiste Faddoul. 2018. Chargrid: Towards understanding 2d documents. *arXiv preprint arXiv:1809.08799* (2018).
- [30] Mohammed Kayed and Chia-Hui Chang. 2009. FiVaTech: Page-level web data extraction from template pages. *IEEE transactions on knowledge and data engineering* 22, 2 (2009), 249–263.
- [31] Vu Le and Sumit Gulwani. 2014. Flashextract: A framework for data extraction by examples. In *Proceedings of the 35th ACM SIGPLAN Conference on Programming Language Design and Implementation*. 542–553.
- [32] Wei Liu, Xiaofeng Meng, and Weiyi Meng. 2009. Vide: A vision-based approach for deep web data extraction. *IEEE transactions on knowledge and data engineering* 22, 3 (2009), 447–460.
- [33] Shangbang Long, Siyang Qin, Dmitry Pantelev, Alessandro Bissacco, Yasuhisa Fujii, and Michalis Raptis. 2022. Towards end-to-end unified scene text detection and layout analysis. In *Proceedings of the IEEE/CVF Conference on Computer Vision and Pattern Recognition*. 1049–1059.
- [34] Navonil Majumder, Soujanya Poria, Alexander Gelbukh, and Erik Cambria. 2017. Deep learning-based document modeling for personality detection from text. *IEEE intelligent systems* 32, 2 (2017), 74–79.
- [35] Oshri Naparstek, Ophir Azulai, Inbar Shapira, Elad Amrani, Yevgeny Yaroker, Yevgeny Burshtein, Roi Pony, Nadav Rubinstein, Foad Abo Dahood, Orit Prince, et al. 2024. KVP10k: A Comprehensive Dataset for Key-Value Pair Extraction in Business Documents. In *International Conference on Document Analysis and Recognition*. Springer, 97–116.
- [36] Feng Niu, Che Zhang, Christopher Ré, and Jude W Shavlik. 2012. DeepDive: Web-scale Knowledge-base Construction using Statistical Learning and Inference. *VLDB* 12 (2012), 25–28.
- [37] Nerya Or and Shlomo Urbach. 2021. Few-shot learning for structured information extraction from form-like documents using a diff algorithm. In *Proc. Document Intell. Workshop KDD*.
- [38] Shubham Singh Paliwal, D Vishwanath, Rohit Rahul, Monika Sharma, and Lovekesh Vig. 2019. Tablenet: Deep learning model for end-to-end table detection and tabular data extraction from scanned document images. In *2019 International Conference on Document Analysis and Recognition (ICDAR)*. IEEE, 128–133.
- [39] Aditya Parameswaran, Nilesh Dalvi, Hector Garcia-Molina, and Rajeev Rastogi. 2011. Optimal schemes for robust web extraction. In *Proceedings of the VLDB Conference*, Vol. 4. VLDB Endowment.
- [40] Suresh Parthasarathy, Lincy Pattanaik, Anirudh Khatri, Arun Iyer, Arjun Radhakrishna, Sriram K Rajamani, and Mohammad Raza. 2022. Landmarks and regions: a robust approach to data extraction. In *Proceedings of the 43rd ACM SIGPLAN International Conference on Programming Language Design and Implementation*. 993–1009.
- [41] Akshay Gadi Patil, Omri Ben-Eliezer, Or Perel, and Hadar Averbuch-Elor. 2020. Read: Recursive autoencoders for document layout generation. In *Proceedings of the IEEE/CVF Conference on Computer Vision and Pattern Recognition Workshops*. 544–545.
- [42] Sunita Sarawagi et al. 2008. Information extraction. *Foundations and Trends® in Databases* 1, 3 (2008), 261–377.
- [43] Ritesh Sarkhel and Arnab Nandi. 2021. Improving information extraction from visually rich documents using visual span representations. *Proceedings of the VLDB Endowment* 14, 5 (2021).
- [44] Štěpán Šimsa, Milan Šulc, Michal Uříčář, Yash Patel, Ahmed Hamdi, Matěj Kocián, Matyáš Skalický, Jiří Matas, Antoine Doucet, Mickaël Coustaty, et al. 2023. Docile benchmark for document information localization and extraction. In *International Conference on Document Analysis and Recognition*. Springer, 147–166.
- [45] Carlos Soto and Shinjae Yoo. 2019. Visual detection with context for document layout analysis. In *Proceedings of the 2019 Conference on Empirical Methods in Natural Language Processing and the 9th International Joint Conference on Natural Language Processing (EMNLP-IJCNLP)*. 3464–3470.
- [46] Zineng Tang, Ziyi Yang, Guoxin Wang, Yuwei Fang, Yang Liu, Chenguang Zhu, Michael Zeng, Cha Zhang, and Mohit Bansal. 2023. Unifying vision, text, and layout for universal document processing. In *Proceedings of the IEEE/CVF conference on computer vision and pattern recognition*. 19254–19264.
- [47] Sandeep Tata, Navneet Potti, James B Wendt, Lauro Beltrao Costa, Marc Najork, and Beliz Gunel. 2021. Glean: Structured extractions from templatic documents. *Proceedings of the VLDB Endowment* 14, 6 (2021), 997–1005.
- [48] Yiheng Xu, Minghao Li, Lei Cui, Shaohan Huang, Furu Wei, and Ming Zhou. 2020. Layoutlm: Pre-training of text and layout for document image understanding. In *Proceedings of the 26th ACM SIGKDD international conference on knowledge discovery & data mining*. 1192–1200.
- [49] Yiheng Xu, Tengchao Lv, Lei Cui, Guoxin Wang, Yijuan Lu, Dinei Florencio, Cha Zhang, and Furu Wei. 2022. XFUND: a benchmark dataset for multilingual visually rich form understanding. In *Findings of the Association for Computational Linguistics: ACL 2022*. 3214–3224.
- [50] Xiao Yang, Ersin Yumer, Paul Asente, Mike Kralej, Daniel Kifer, and C Lee Giles. 2017. Learning to extract semantic structure from documents using multimodal fully convolutional neural networks. In *Proceedings of the IEEE conference on computer vision and pattern recognition*. 5315–5324.
- [51] Yang Yang, Zhilei Wu, Yuexiang Yang, Shuangshuang Lian, Fengjie Guo, and Zhiwei Wang. 2022. A survey of information extraction based on deep learning. *Applied Sciences* 12, 19 (2022), 9691.